NISTIR 6324

THE ZONE FIRE MODEL JET: A MODEL FOR THE PREDICTION OF DETECTOR ACTIVATION AND GAS TEMPERATURE IN THE PRESENCE OF A SMOKE LAYER

William D. Davis

NIST

THE ZONE FIRE MODEL JET: A MODEL FOR THE PREDICTION OF DETECTOR ACTIVATION AND GAS TEMPERATURE IN THE PRESENCE OF A SMOKE LAYER

William D. Davis
Building and Fire Research Laboratory
National Institute of Standards and Technology
Gaithersburg, Maryland 20899

May 1999

CONTENTS

i

ACKNOWLEDGMENTS

THE ZONE FIRE MODEL JET

A MODEL FOR THE PREDICTION OF DETECTOR ACTIVATION AND GAS TEMPERATURE IN THE PRESENCE OF A SMOKE LAYER

William D. Davis

Abstract

The zone model JET is a two-zone, single compartment computer model designed to predict the plume centerline temperature, the ceiling jet temperature and the ceiling jet velocity produced by a single fire plume. The impact on the upper layer due to the presence of draft curtains, ceiling vents and thermal losses to the ceiling are included in the model. Ceiling mounted fusible links and link actuated ceiling vents can be included in the model calculations. The unique feature of this model is that the characteristics of the ceiling jet depend on the depth of the hot layer.

1.0 Overview of JET

The zone model JET evolved from the computational platform used for the zone model LAVENT [1] and therefore contains many of the features found in LAVENT. The major differences between JET and LAVENT include the ceiling jet temperature and velocity algorithms, the fusible link algorithm, and the use of a variable radiative fraction as a function of fire size and type. A new input module has been designed which allows the program to operate in the Windows environment.

JET is a two-zone, single compartment model where each zone or layer is assumed to be uniform in density and temperature. The temperature and density of the upper layer responds to a growing fire while the lower layer is assumed to remain at ambient temperature and pressure. A fire driven ceiling jet is assumed to flow along the flat ceiling.

The compartment is rectangular in plan and is enclosed by a combination of walls and draft curtains. The ceiling contains fusible links which may be associated with ceiling vents where the ceiling vents operate in response to the fusing of the links. The fusible links are heated convectively by the ceiling jet and cooled by conduction to the structural supports supporting the links. The ceiling vents remove upper layer gas from the compartment. The impact of a ceiling vent on the local temperature and velocity of the ceiling jet is neglected.

The fire is characterized by a time dependent heat release rate, HRR, a time dependent radiative fraction, and either a constant fire diameter or a variable fire diameter which is determined using a HRR per unit area for the burning material.

1.1   Scope of Application

Applications that are appropriate for Jet include:

   a. determination of activation times for fusible links controlling vents and sprinklers in compartments bounded by walls, draft curtains, or combinations of walls and draft curtains for user defined fire sizes and growth rates. Compartments with one or more sides unbounded may also be modeled,

   b. determination of the impact of draft curtains and ceiling vents on the depth of the smoke layer and the activation of fusible links,

   c. determination of maximum ceiling temperature as a function of upper layer depth and temperature with or without ceiling vents, and

   d. determination of maximum ceiling jet temperature and ceiling jet velocity as a function of upper layer depth and radial distance from the plume centerline with or without ceiling vents.

JET is a two zone compartment model and therefore contains several assumptions that are typical of this approximation scheme [2]. Specific assumptions which the user must remember in order to use JET successfully include: the compartment pressure remains near ambient, the fire is fully ventilated, the flames from the fire do not touch the ceiling, and the fire is always located near the center of the compartment or curtained area. Violation of any of these conditions may make the results of JET invalid.

Based on comparisons to experimental data found later in this paper, the predictions of JET generally agreed with experimental results for compartments with ceiling heights up to 22 m. JET may continue to perform well at ceiling heights greater than 22 m but there has been no experimental comparisons at these greater heights.

1.2   Physical Models

The basic differential equations used to calculate the changing conditions of the upper layer are based on the conservation of upper layer mass,

$$dm/dt = \sum dm_i/dt \qquad (1)$$

and upper layer energy

$$d[(y_c - y)\rho T A c_v]/dt = \sum \dot{q}_i + pA dy/dt \qquad (2)$$

where dm_i/dt is the mass flow rate to the upper layer, y_c is the ceiling height, y is the height to the bottom of the upper layer, ρ is the upper layer gas density, T is the upper layer gas temperature, A is the ceiling area, p is the absolute pressure at the layer interface, c_v is the specific heat at constant volume, $\dot{q}_i$ is the enthalpy flow rate to the upper layer, and t is time.

Using the ideal gas law, equation 2 can be rewritten as

$$dy/dt = -\sum \dot{q}_i / (A c_p \rho_\infty T_\infty) \tag{3}$$

where ρ_∞ is the ambient density, T_∞ is the ambient temperature, and c_p is the heat capacity at constant pressure. Equations 1 and 3 are the differential equations used to calculate the mass and layer height of the upper layer.

Mass and enthalpy flow into or out of the upper layer comes from the plume, ceiling vents and flow under the draft curtains. In addition, heat is transferred out of the layer to the ceiling through convection. The ceiling is also heated through radiation from the fire. For the radiation calculation, the fire is assumed to be a point source and absorption and radiation from the compartment gases is assumed to be negligible. This last assumption will be satisfied whenever layer heating by radiation from the fire is small compared to the convective heat release rate of the fire and convective heat losses to the ceiling dominate the thermal losses from the layer. The algorithms used for these calculations are identical to the algorithms used in LAVENT and are documented in reference [3].

The plume centerline temperature is calculated using the method of Evans [4]. When an upper layer is not present, the modified correlation of Heskestad and Delicatsios [5] is used to compute the excess plume centerline temperature, ΔT_p, using the correlation

$$\Delta T_p = 9.28 T_\infty ((1-\chi_r)\dot{Q})^{2/3} / (\rho_\infty c_p T_\infty g^{1/2} H^{5/2})^{2/3} \tag{4}$$

where χ_r is the radiative fraction of the fire, $\dot{Q}$ is the heat release rate of the fire (HRR), g is the acceleration of gravity, and H is the height of the ceiling above the fire surface. At a temperature of 20 °C, equation 4 becomes:

3

$$\Delta T_p = 25.5 \frac{((1-\chi_r)\dot{Q})^{2/3}}{H^{5/3}} \tag{5}$$

The coefficient 25.5 is consistent with the 26.0 value recommended by Beyler [6] based on a survey of plume centerline temperature experiments.

When an upper layer forms, this correlation must be modified in order to correctly predict plume centerline temperature since the plume now includes added enthalpy by entraining hot layer gas as it moves through the upper layer to the ceiling. Evans' method defines the strength $\dot{Q}_I^*$ and location Z_I of a substitute source as seen in the upper layer by

$$\dot{Q}_{I,2}^* = [(1 + C_T \dot{Q}_{I,1}^{*2/3})/\xi C_T - 1/C_T]^{3/2} \tag{6}$$

and

$$Z_{I,2} = [\frac{\xi \dot{Q}_{I,1}^* C_T}{\dot{Q}_{I,2}^{*1/3}[(\xi-1)(\beta^2+1) + \xi C_T \dot{Q}_{I,2}^{*2/3}]}]^{2/5} Z_{I,1} \tag{7}$$

where I refers to the layer interface, 1 and 2 refer to the lower and upper layer respectively, ξ is the ratio of upper to lower layer temperature, β is the velocity to temperature ratio of Gaussian profile half widths ($\beta = 0.9555$), and $C_T = 9.115$ and

$$\dot{Q}_{i,1}^* = \frac{(1-\chi_r)\dot{Q}}{(\rho_\infty c_\infty T_\infty g^{1/2} Z_{i,1}^{5/2})} \tag{8}$$

The new ceiling height, H_2, is then obtained from

$$H_2 = H_1 - Z_{I,1} + Z_{I,2} \tag{9}$$

where $Z_{I,1}$ is the height from the fire to the layer interface and H_1 is the height of the ceiling above the fire. The new values of the fire source and ceiling height with T_∞ equal to the upper

layer temperature are then used in equation 4 to obtain the plume centerline temperature as suggested in Evans' paper. The algorithms used for the layer depth and temperature calculations were taken from LAVENT after modification to include a user determined radiative fraction as a function of HRR.

The ceiling jet temperature is calculated using the following model. When an upper layer is absent, the ceiling jet temperature excess ΔT_{cj} is calculated using the radial dependence of the ceiling jet temperature from Alpert's correlation [7]

$$\Delta T_{cj} = 0.68 \Delta T_p / r^{2/3} \tag{10}$$

for $r/H > 0.18$. Here, r is the radial distance from the plume centerline. As an upper layer develops, the ceiling jet temperature excess as a function of radius for $r/H > 0.18$ is calculated using the correlation of Davis et. al. [8]

$$\Delta T_{cj} = C/r^{\gamma} \tag{11}$$

$$C = \beta r_o^{\gamma} \Delta T_p \tag{12}$$

where

$$\beta = (0.68 + 0.16(1 - e^{-y_L/y_j})) \tag{13}$$

$$r_o = 0.18H \tag{14}$$

$$\gamma = 2/3 - \alpha(1 - e^{y_L/y_j}) \tag{15}$$

and $\alpha = 0.44$, $y_j = 0.1*H$, y_L is the layer thickness, and ΔT_p is the plume centerline temperature excess as calculated using Evans' method (equations 3-5 & 7-8). The value of α is determined

by the requirement that with no hot layer, the radial dependence on the ceiling jet temperature should follow Alpert's value of 2/3, while after the layer forms, the radial dependence will be reduced to a minimum of 0.23 as the layer depth increases.

JET's ceiling jet velocity calculation uses Alpert's correlation [7] when no layer is present. As a layer forms, the ceiling jet velocity, v_{cj}, reduces as a function of layer depth using the following relationship.

$$v_{cj} = 0.195 * ((1 - \chi_r) * \dot{Q})^{1/3} H^{1/2} * (1 - 0.25 * (1 - e^{y_L/y}))/r^{5/6} \qquad (16)$$

for $r/H > 0.18$. The reduction of ceiling jet velocity as the upper layer forms has been demonstrated in the experiments by Montevalli et al. [9].

The equation governing the heating of the fusible links is given by [10]

$$\frac{dT_{lk}}{dt} = \frac{\sqrt{v_{cj}}}{RTI}(T_{cj} - T_{lk} - \frac{C}{\sqrt{v_{cj}}}(T_{lk} - T_\infty)) \qquad (17)$$

Here T_{lk} is the link temperature, T_{cj} is the ceiling jet temperature at the link, and RTI is the response time index of the link. The constant C represents the geometry and material properties associated with the conductive heat losses from the link to the supporting structure. The default value used by the program is 0.5. An assumption used in this equation is that the supporting structure remains at ambient temperature, T_∞. This will only be a good approximation early in the fire simulation. As the upper layer heats up the supporting structure, heat transfer to the support from the sprinkler link will be reduced and the algorithm will begin to overestimate heat loss. Since the thermal inertia of the supporting structure is large compared to the thermal inertia of the fusible link, this effect will only be important for threshold activations where the time to activation becomes substantial.

2.0 Using JET

The program JET has a User Interface (UI), jet.exe, written in MICROSOFT VISUAL BASIC 4.0* which allows the user to create or edit input files and to run JET. The program JET,

---

*Certain trade names are identified to specify the software used. In no case does such identification imply recommendation or endorsement by the National Institute of Standards and Technology, nor does it imply that the products are necessarily the best available for the purpose.

jetvb1.exe, is written in FORTRAN 77 and is compiled using DIGITAL VISUAL FORTRAN**.
A default data file, default.dat, is included. Jet.exe, jetvb1.exe, default.dat,Vfp6r.dll and
Vfp6renu.dll should be copied into a directory with a path name c:\jet.

To run JET, the user enters c:\jet\jet or double clicks on the file jet.exe in the directory c:\jet.
The user interface should appear on the screen. The interface has a menu at the top of the screen
and a set of five buttons which provide the user with the initial options to use JET. Click on the
button labeled **Open File** and select the jet directory and the default.dat file. Values should
appear in the windows of the UI which represent the values for the default case. The first time
you use JET, you should run the default case. To do this, click the button **Run Jet**. You will be
prompted to enter an input file and to run the default case, type c:\jet\default.dat. The next
prompt will be for an output file which could be c:\jet\default.out or any other name and path you
choose. The final prompt will create a spreadsheet file and you could choose c:\jet\default.gph or
any other name and path. The program will then run and when it is finished, you will be back in
the user interface. The output file may be examined by using NOTEPAD, WORDPAD, the DOS
editor or any other ASCII editor. The spreadsheet file may be opened by any spreadsheet
software which imports space delimited columns of numbers. The default output is in the
appendix and should be compared with the output just generated.

Using the UI, change some of the values in the default file by clicking on the value to be changed
and then entering a new value. Use the menu selections at the top of the UI to add or delete
vents, links or fire segments. Each of these inputs will be explained in detail in the next section.
Save your changes in a different file and path and rerun JET.

3.0   The User Interface

The UI has been designed to provide a complete display of an input file on one computer screen.
For each value of input, the units for that input are clearly displayed with the input value. The
user must use the same type of units when entering new numbers for a particular input value.
The following will be a short description of the function of each button, menu selection, or input
value found on the UI.

3.1   Buttons

Open File   When this button is clicked, a prompt appears for a path and file name. To enter
the default file, type c:\jet\default.dat. The path must be included with the file
name. A new file may be entered using this option even though a file is already
displayed by the interface. The new file values will overwrite the present values

---

**Certain trade names are identified to specify the software used. In no case does such
identification imply recommendation or endorsement by the National Institute of Standards and
Technology, nor does it imply that the products are necessarily the best available for the purpose.

on the interface. **The user should save the present file before entering a new file on the interface as any changes to the present file will be lost when the new file values are entered.**

Unit Convert This button is used to convert the UI display from SI units to English units or English units to SI units.

Save File When this button is clicked, a prompt appears for a path and file name. The path must exist for a file to be saved using this button.

Run Jet When this button is clicked, a prompt appears for a path and file name for first an input file, an output file and then a spreadsheet file. Once these entries are made, JET will run using the data from the input file. When the program has completed, control will return to the UI.

End Clicking this button will end the UI session.

3.2   Menus

Vents Choosing this selection allows the user to add or remove ceiling vents from the simulation. To add a vent, choose the add option of the vent selection. There will be prompts for the ceiling vent area and for the fusible link number which will identify the link controlling the vent opening. Each fusible link was assigned a number when the link properties were entered. Each vent is automatically assigned a number when the vent properties are entered. To remove a vent, choose the remove option and enter the vent number to be removed or click on the vent number.

Fire Choosing this selection allows the user to add or remove fire segments from the simulation. The fire in JET is simulated by a series of linear segments which define the HRR and radiative fraction of the fire as a function of time. To add a segment, choose the add option and enter the time, HRR, and radiative fraction as prompted (see reference [8] for a discussion of the importance of radiation fraction). The program will linearly interpolate between this point and adjacent points. To delete a segment, choose the delete option and enter the number of the segment to be deleted. A fire segment may also be deleted by clicking on the segment number. The maximum number of segments is restricted to 10.

Links Choosing this selection allows the user to add or remove links from the simulation. To add a link, choose the add option and enter the temperature at which the link activates, the RTI of the link, the radial distance of the link from the center of the plume, the distance that the link is located beneath the ceiling and the C-factor for the link. The present simulation does not use the distance that the

8

link is located beneath the ceiling but the data is included for future development. A number will be assigned to represent the new link. To remove a link, choose the remove option and enter the link number to be removed. A link may also be removed by clicking on the link number. If the link is used to simulate sprinkler activation, the algorithm will allow the user to determine when a sprinkler will activate but does not include the impact of the sprinkler spray on subsequent activations.

3.3   Input Values

The following is a short description of each input value shown on the UI. Each selection is shown as a two column entry. The left column names the entry and the right column gives the present value for the entry. The present value can be changed by clicking either the right or left column and entering a new value in the input box which appears on the screen.

Room Geometry

The dimensions of the fire room are specified in this section with the size of the rectangular floor given using the room length and room width selections and the height of the ceiling above the floor using the ceiling height selection. Draft curtains can bound either a portion of the perimeter of the room or the entire perimeter. The Draft curtains are specified by the curtain length and curtain height entries. The curtain height entry refers to the height of the bottom of the draft curtain above the floor and curtain length entry specifies the length of the curtain. To surround the entire area with a draft curtain, the curtain length should equal the perimeter of the room. Any part of the perimeter length that is not part of the draft curtain is assumed to be solid wall. A room with a door may be simulated by representing the door width with a curtain length and the height of the top of the door with a curtain height.

Ceiling Properties

This section allows the user to specify the thermal properties of the ceiling material and the thickness of the ceiling. The user may access a small material data base by clicking on the blank entry to the right of MATERIAL. For special materials, the user may enter the thermal conductivity, heat capacity and density by clicking on the value in the right column of each named entry and entering a new value. The thickness of the ceiling material may also be entered by the user.

Fire Properties

Program inputs specified in this section include the ambient temperature which is the temperature of the lower layer, the height of the fire above the floor and the fire diameter. The fire diameter can be specified in two separate ways. If the fire is known to have a constant diameter, the user should click yes to the prompt to use a constant fire diameter and enter the

diameter. Otherwise, the user will specify a HRR/area for the fire. This may be done by referring to the HRR/area database and entering a HRR/area for the fire in question. The database will appear in a box in the lower left hand corner of the UI.

Link Inputs

Each fusible link is referred to by an automatically assigned link number, a radial distance from the plume centerline, an RTI or response time index which is a measure of the thermal lag in the link, a fuse temperature which is the temperature at which the link activates, a C-factor which is a measure of the heat loss of the link to its supporting structure, and a distance that the link is located beneath the ceiling. The distance that the link is located beneath the ceiling is not presently used and is given a default value. The present algorithm assumes that the link is located in the hottest part of the ceiling jet.

Fire Inputs

Fire inputs include an automatically assigned segment number, the time that the fire has that particular HRR, and the radiative fraction of the fire at that time. JET will take this input data and construct linear fits for both the HRR and the radiative fraction between time adjacent segments.

Vent Inputs

Vent inputs include a computer assigned vent number, the area of the ceiling vent and the link number which designates which link will control the opening of the vent.

Program Times

Program times include the Output Time which sets the time interval used by the program to write results to the output file and the End Time which represents the last time calculated by JET before the program terminates.

Option Inputs

In general, the user should not change any of these options unless JET is not able to generate a solution for a particular set of input values. The following discussion of how JET arrives at a solution will be useful to the user desiring to change any of these options.

Jet uses a differential equation solver, DDRIVE2, to solve the set of differential equations associated with the conservation of mass and energy equations and the equations describing the temperatures of the fusible links. A Gauss-Seidel/Tridiagonal solver using the Crank-Nicolson formalism is used to solve the set of partial differential equations associated with the heat conduction through the ceiling. Since two different solvers are being used in JET, there is

potential for the solvers to become incompatible with each other, particularly if the upper layer has nearly reached a steady-state temperature but the ceiling is still increasing it's temperature. When this occurs, the differential equation solver will try to take time steps that are too large for the Gauss-Seidel solver to handle and a growing oscillation in the ceiling temperature variable may occur. By decreasing the flux-update interval, the growing oscillation may be suppressed. The smaller the flux-update interval, the slower JET will run.

The Gauss-Seidel Relaxation Coefficient may be changed to speed up JET or to handle a case that will not run with the present coefficient. Typical values of this coefficient range between 0.2 and 1.0.

The tolerances for both solvers may be changed. Increasing the values may produce a quicker calculation while decreasing the values may increase the accuracy of the calculation. If the tolerance values are made too small, the program will either run very slowly or not run at all. Suggested tolerances would be in the range of 10^{-5} to 10^{-6}.

The DDRIVE2 solver has three options which it uses to arrive at a solution. When the solver type input is set at 1, 2 or 3, DDRIVE2 uses a nonstiff method, a stiff method or the solver determines which method to use respectively. For the equations used in JET, calculations will run much faster using the nonstiff setting. Additional information concerning stiff solvers may be found in reference [2].

4.0   Comparison of Jet Predictions with Experiments

This section includes the results of a number of simulations of fire experiments. The purpose of this section is to provide the user with some insight as to accuracy and limitations of JET as a predictive tool.

4.1   Ceiling height of 0.58 m

A cylindrical enclosure of 1.22 m diameter formed by a 0.29 m deep PMMA curtain around a 13 mm thick ceramic fiber board ceiling was used to study the temperature produced by an axisymmetric plume. The fire source was a methane gas burner of diameter 0.0365 m located at the center of the cylinder. The top of the burner was located 0.58 m beneath the ceiling. The heat release rate was 0.62 kW. Details of this experiment are available in reference [11].

This experiment measured plume centerline temperature as a function of height but not ceiling jet temperature. Figure 1 compares the predicted plume centerline temperature at the ceiling impingement point with the measured value. Uncertainty intervals for the measurements were given in the reference while the uncertainty in the calculations represent an estimation of the uncertainty in the HRR of the experiment of ±5%. The plume centerline temperature predicted using JET lies within the combined uncertainty interval of the measurement and the calculation.

4.2 Ceiling height of 1.0 m

A cylindrical enclosure of diameter 2.13 m formed by a 0.5 m deep corrugated cardboard curtain around a 1.27 cm thick fiberboard ceiling was used to study the development of a ceiling jet at distances of $r/H = 0.26$ and $r/H = 0.75$ where r is the radial distance from the fire center and H is the distance between the burner outlet and the ceiling. The fire consisted of a methane flame produced using a 2.7 cm diameter burner. The burner outlet was located at the center of the cylindrical enclosure and was 1.0 m below the ceiling. The fire sizes used in this study were 0.75 kW and 2.0 kW. Additional details concerning this experiment can be found in reference [9].

Figures 2 and 3 gives the predictions of JET compared with the ceiling jet temperature maximums measured at $r/H = 0.26$ and $r/H = 0.75$. There was no guidance given by the authors concerning the uncertainties of their measurements. It was assumed that an error interval of ±10% would be a reasonable approximation of the measurement accuracy which would include systematic errors and data scatter in the temperature measurements, the burner flow rates, combustion efficiency, and radiative fraction of the fuel source. JET underpredicted the ceiling jet temperature for both radial positions for the 2.0 kW fire and underpredicted the ceiling jet temperature at $r/H = 0.26$ for the 0.75 kW fire. JET predicted the ceiling jet temperature at $r/H = 0.75$ for the 0.75 kW fire within the combined uncertainty of the measurement and calculation.

4.3 Ceiling Height of 2.7 m

A series of experiments were conducted using a free-hung ceiling measuring 9.75 m x 14.6 m. Simulated beams, 0.305 m deep and separated by 1.22 m, were installed on the ceiling with the beams parallel to the long dimension of the ceiling. A pair of experiments (tests 7 & 4), one with a 1.22 m deep draft curtain and one without a draft curtain, were chosen for the analysis. Wood cribs were used as the fire source with the bottom of the beams located 2.43 m above the top of the Wood cribs. Since the growth rate of the fire as a function of time was provided, comparisons were made at several different fire sizes. The fire sizes for these comparisons ranged from 30 kW to 830 kW. Additional information concerning the experiments can be found in reference [12].

Figure 4 and 5 display the comparison between the predictions of JET and the measurements for the plume centerline temperature for test 4 which contained 0.305 m deep beams and test 7 which included the ceiling beams plus a 1.22 m deep draft curtain. The uncertainty intervals used for the data are estimated to be ±5% while the calculations were done by taking the reported time dependent heat release rate and varying the radiative fraction between 0.20 and 0.45. The temperatures are calculated using a radiative fraction of 0.35. JET provided predictions within the combined uncertainty intervals for the smaller fire sizes (early times) but underpredicted the temperature for the large fires.

Several reasons may combine to produce the significant underprediction at the largest fire sizes

for these experiments. First, the combustion region of the flame is approaching the ceiling for the larger fires. The plume algorithms used in these comparisons are valid only out of the combustion region and hence when the flames get close to the ceiling, the accuracy of the plume algorithm comes into question. Second, since the combustion region is close to the ceiling, the radiation to the ceiling and hence to the thermocouple becomes significant. The thermocouple measurements may require correction for radiation effects which would effectively lower the measured temperature. This was not done in the experiments. Third, as the fire size increases, the radiative fraction should decrease with fire size as the fire volume becomes optically thick. The decreasing radiation fraction with fire size is difficult to estimate theoretically and was not included in the calculations.

4.4   Ceiling Height of 10 m

A series of experiments were conducted in a building with a space of 53 m x 22 m x 11.3 m high. A 2 m square hexane fire produced a steady-state heat release rate of 4.6 MW. The convective heat release rate was estimated to be 3.05 MW. The roof was carried on 1 m deep timber beams and a draft curtain 3.2 m deep as measured from the bottom of the beams divided the building into two spaces. A false level ceiling 10 m above the floor was attached to the bottom of the beams in the space where the experiments were conducted. Additional information concerning the experiments can be found in reference [13].

Shown in figure 6 are comparisons of the estimated plume centerline temperature to the predictions of JET. The uncertainties for the radial temperature measurements, as provided by the authors, was ± 4°C. The uncertainties for the calculations are based on the assumption that the radiative fraction of the fuel varied from 0.25 to 0.40. The calculated values are based on a radiative fraction of 0.34, which was given by the authors. From the figure, JET overpredicts the plume centerline temperature. One explanation for this result is that the experiment may not have had enough thermocouples in the plume region to resolve the plume centerline temperature. It was noted that the plume centerline wandered in location and typically was located some distance away from the fire centerline. The plume centerline temperature value used in this comparison was extrapolated from a radial temperature dependence plot which did not include a temperature at the plume centerline. The extrapolation was fairly flat in temperature which suggests that the plume centerline temperature used for this experiment was lower than actually produced by the experiment.

Figure 7 gives the comparison between the measured values and the ceiling jet temperature predictions of JET. The values predicted by JET lie within the combined uncertainty interval of the measurements and the calculations.

4.5   Ceiling Height of 15 m

A series of JP-5 pool fires were conducted in a hangar of size 97.8 m x 73.8 m x 15.1 m. The fires were centered under a draft curtained area 18.3 m x 24.4 m with a ceiling height of 14.9 m.

The draft curtain was 3.7 m deep. Three JP-5 pool fire experiments, a 0.61 m square 0.48 MW fire, a 1.5 m diameter 2.8 MW fire and a 2.5 m diameter 7.7 MW fire, were modeled. Additional information concerning these experiments can be found in reference [14].

Figure 8 gives the comparisons of the plume centerline temperature predictions of JET and the measured values. JET predicts the temperature within the uncertainty intervals for the two smaller fires. The heat release rate for the 7.7 MW fire was determined by a fuel mass loss method rather than direct load cell measurements which, due to fuel evaporation at the end of the experiment, may lead to an overestimation of HRR but there was no way to determine how much of an overestimate is involved in the measurement.

The uncertainty interval for the measurements were based on the measured RMS temperature fluctuations and are equal to $\pm\sigma$. The uncertainty interval for the calculations was determined by varying the HRR $\pm15\%$. This uncertainty should include the uncertainty in the radiative fraction as well as the uncertainty in the HRR. The uncertainty in the HRR was not increased for the 7.7 MW fire.

Figures 9 and 10 give the comparisons of the ceiling jet temperature predictions of JET with the measured values. Only the 2.7 MW fire and the 7.7 MW were used in the comparison owing to the small temperature excess in the ceiling jet for the 0.48 MW experiment. The temperature predictions of JET were within the combined uncertainty interval for all radial positions for the 2.7 MW experiment and for the 3.1 m position in the 7.7 MW experiment. The temperatures at the 6.1 m and 9.1 m positions for the 7.7 MW fire were overpredicted by JET.

4.6   Ceiling Height of 22 m

A series of JP-5 and JP-8 pool fires were conducted in a hangar of size 73.8 m x 45.7 m and had a barrel roof which was 22.3 m high at the center and 12.2 m high at the walls. Corrugated steel draft curtains were used to divide the ceiling into five equal bays approximately 14.8 m x 45.7 m with the fire experiments conducted in the middle bay and centered under the 22.3 m high ceiling. Nine experiments with fire sizes ranging from 1.4 MW to 33 MW were modeled. The location of the fire plume at the center of the building allowed JET to be applied to these tests as the shape of the ceiling near the center of the building was relatively flat. Additional information concerning these experiments can be found in reference [14].

Figure 11 gives the comparison of the plume centerline temperature predictions of JET with the measured values. The predictions of JET were within the uncertainty intervals for all the experiments. The uncertainty intervals for the measurements were based on the measured RMS temperature fluctuations and are equal to $\pm\sigma$. The uncertainty interval for the calculations was determined by varying the HRR $\pm15\%$. This uncertainty should include the uncertainty in the radiative fraction as well as the uncertainty in the HRR.

Figures 12 - 18 give the comparison of the ceiling jet temperature predictions of JET with the

14

measured values at distances of 6.1 m, 9.1 m, and 12.2 m from plume center. These measurements were along the curved part of a barrel roof. With the exception of the 6.1 m position of the 4.9 MW fire, all the predictions of JET were within the uncertainty interval for the measured values. The uncertainty intervals for the ceiling jet temperatures were treated in the same manner as for the plume centerline temperatures.

5.0   Sprinkler Activation Simulations

Simulating sprinkler activation requires good predictive capabilities for the ceiling jet temperature and velocity as well as knowing the thermal response of the sprinkler bulb or fusible link and the associated heat losses from the sprinkler bulb or fusible link to the piping connecting the link to the water supply. The prediction of activation times become more uncertain as the conditions at the sprinkler approach a threshold activation situation. In this instance, the accurate location of the plume centerline at the ceiling becomes important and this location is typically not accurately known due to plume motion and the lack of a sufficiently fine grid of thermal sensors at the ceiling.

For the experiments discussed below, the uncharged sprinkler system did not discharge water when activations occurred and therefore the experimental results do not include the impact of sprinkler spray on sprinklers located down stream from the first sprinkler that activated. The sprinklers were quick response type with response time index or RTI of 35 $(m\ s)^{1/2}$ and activation temperature of 79 °C.

The predictions of JET, using a C factor of 0.5 for the sprinklers, are compared with the time of first activation of a sprinkler at a given radial position from the plume centerline. Uncertainties are not given for these comparisons as the value of the C factor as well as the uncertainty in RTI for these sprinklers is not known. Based on the temperature profile at the ceiling, it was assumed that the HRR increased linearly to maximum value 50 s after the full pan surface was covered with flame.

5.1   Activation with a 15 m Ceiling

Figure 19 shows the predicted and measured dry sprinkler activation times as a function of radius from the plume centerline for a 7.7 MW JP-5 pan fire. The sprinklers activated at 79 °C and had a response time index, RTI, of 35 $(m\ s)^{1/2}$. Agreement with experiment is within 25 % for the fusible links located at 3 m and 6.1 m. At 9.1 m, JET predicted no activation but the sprinkler did activate at a time when the entire hangar was filling with smoke which would make the layer much deeper than calculated in JET. The JET calculation simulated only the draft curtained area and therefore limited the smoke layer to be no deeper than would be produced by draft curtains.

5.2   Activation with a 22 m Ceiling

Figures 20 - 23 show the predicted and measured dry sprinkler activation times as a function of

15

radius from the plume centerline for JP-5 pan fires of fire size 14.3 MW, 14.6 MW, 15.7 MW and 33 MW. The sprinklers activated at 79 °C and had a RTI, of 35 $(m s)^{1/2}$. Agreement with experiment is within 25 % for all the predictions where sprinklers activated in less than 200s except for the 6.1 m location for the 14.3 MW fire and the 9.1 m location for the 33 MW fire. The lack of agreement at the 9.1 m position for the 33 MW fire may be due to an RTI or C factor which is larger than average as the activation of sprinkler links on either side of this link were predicted within 20 %. Sprinklers which activated after 200 s at the 9.1 m and 12.2 m positions were not predicted to activate by JET. The activation of these sprinklers are close to threshold and the prediction of threshold events requires accurate knowledge of the sprinkler C factor which was not available for these comparisons. Another factor which is important in threshold events is the movement of the plume near the ceiling which can cause sprinklers to activate as the plume sways toward the sprinkler. Plume sway is not included in a zone model calculation.

6.0   Summary

Figures 24-26 provide a summary of the predictions of JET to the experimental measurements. The results presented on the figures are percent differences between the prediction value and measurement value divided by the measurement value. For temperature comparisons, a 20% or less difference would represent a result which would lie either close to or within the combined uncertainties of the measurements and the predictions. For sprinkler comparisons, a 25 % or greater combined uncertainty is warranted due to the need to know the ceiling jet velocity, sprinkler link RTI and the sprinkler C factor in addition to the ceiling jet temperature and HRR. JET predicted the plume centerline temperature to within 20 % for 75 % of the experiments, the ceiling jet temperature to within 20 % for 83 % of the experiments and the sprinkler activation time to within 25 % for 83 % of the experiments for sprinkler locations within 6.1 m of plume center.

Additional testing would be useful to further refine the predictive capabilities of JET. In particular, sprinkler activation needs to be tested at lower ceiling heights and with different fuel types. The algorithm dealing with the reduction of the ceiling jet velocity as a layer forms is based on only a few observations and needs to be verified in a more quantitative manner. The same can be said of the heat conduction part of the sprinkler link algorithm which is based on very little experimental data.

The user applying JET to other fire scenarios should realize that to get the agreement displayed in this paper, the HRR and the radiative fraction as a function of HRR must be known. These parameters, along with ceiling height above the fire, are the most important input parameters for JET and must be known with reasonable accuracy in order to produce good predictive results.

6.1   Availability

JET may be obtained from the NIST/BFRL web site at http://fire.nist.gov. The package retrieved under the name JET contains the program, default file, and a copy of this document.

7.0 References

1. Davis, W. D., and Cooper, L. Y., "Estimating the Environment and the Response of Sprinkler Links in Compartment Fires with Draft Curtains and Fusible Link-Actuated Ceiling Vents - Part II: User Guide for the Computer Code LAVENT," *National Institute of Standards and Technology*, NISTIR 89-4122, 1989, pp. 1-36.

2. Forney, G. P., and Moss, W. F., "Analyzing and Exploiting Numerical Characteristics of Zone Fire Models" *Fire Science & Technology*, 14, 1994, pp. 49 - 60.

3. Cooper, L. Y., "Estimating the Environment and the Response of Sprinkler Links in Compartment Fires with Draft Curtains and Fusible Link-Actuated Ceiling Vents - Theory," *Fire Safety Journal* 16, (1990) pp 137-163.

4. Evans, D. D., "Calculating Sprinkler Actuation Time in Compartments," *Fire. Safety Journal.*, 9, 1985, pp. 147-155.

5. Heskestad, G., and Delichatsios, M. A., "The Initial Convective Flow in Fire," *17th International Symposium on Combustion, Combustion Institute, Pittsburgh* , 1978, pp. 1113-1123.

6. Beyler, C. L., "Fire Plumes and Ceiling Jets," *Fire Safety Journal*, 11, 1986, pp. 53-75.

7. Alpert, R. L., "Calculation of Response Time of Ceiling-Mounted Fire Detectors," *Fire Technology*, 8, 1972, pp. 181-195.

8. Davis, W. D., Notarianni, K. A., and Tapper, P. Z., "An Algorithm for Calculating the Plume Centerline Temperature and Ceiling Jet Temperature in the Presence of a Hot Upper Layer." *National Institute of Standards and Technology*, NISTIR 6178, 1998, pp. 1-23.

9. Motevalli, V., and Ricciuti, C., "Characterization of the Confined Ceiling Jet in the Presence of an Upper Layer in Transient and Steady-State Conditions," *National Institute of Standards and Technology*, NIST-GCR-92-613, 1992, pp. 1-134.

10 Heskestad, G., and Bill, R. G., "Quantification of Thermal Responsiveness of Automatic Sprinklers Including conduction Effects," *Fire Safety J.*, 14, 1988, pp. 113-125.

11. Evans, D. D., "Calculating Fire Plume Characteristics in a Two Layer Environment" *Fire Technology*, 20, No. 3, 1984, pp. 39 - 63.

12. Heskestad, G., and Delichatsios, M. A., "Environments of fire Detectors - Phase II: Effect of Ceiling Configuration. Volume II. Analysis", *National Institute of Standards and*

Technology" NBS-GCR-78-129, 1978, pp. 1 - 100.

13. Hinkley, P. L., Hansell, G. O., Marshall, N. R., and Harrison, R., "Large-Scale Experiments with Roof Vents and Srpinklers Part 1: Temperature and Velocity Measurements in Immersed Ceiling Jets Compared with a Simple Model" *Fire Science & Technology*, Vol. 13, No. 1 & No. 2, 1993, pp. 19 - 41.

14. Gott, J.E., Lowe, D. L., Notarianni, K. A., and Davis W., "Analysis of High Bay Hangar Facilities for Detector Sensitivity and Placement," *National Institute of Standards and Technology*, NIST Technical Note 1423, 1997, pp. 1- 315.

Appendix

The default case is an enclosure with floor dimensions of 20 m x 15 m and a ceiling height of 10 m. A draft curtain of length 40 m encloses part of the area with the remaining area enclosed by walls. The height of the draft curtain is 7.0 m. The ceiling is made up of wood with the ceiling properties listed below. The fire is located at the floor, has a constant diameter of 2.0 m and grows from a HRR of 0.0 kW to a HRR of 4.8 MW in 300 s. The radiative fraction of the fire decreases from 0.45 to 0.25 over the 300 s interval. Four quick response fusible links are positioned at radial distances of 2 m, 4 m, 6 m and 8 m from the fire with the link at 4 m controlling the opening of a 20 m^2 ceiling vent. The program generates an output every 25 s over the 300 s calculation. The program output, default.out, is listed below.

```
CEILING HEIGHT =              10.0 M
ROOM LENGTH =                 20.0 M
ROOM WIDTH =                  15.0 M
CURTAIN LENGTH =              40.0 M
CURTAIN HEIGHT =              7.0 M
MATERIAL =               "WOOD"
CEILING CONDUCTIVITY =    .117E+00 W/M K
CEILING DENSITY =         .400E+03 KG/M3
CEILING HEAT CAPACITY =   .163E+04 J/M K
CEILING THICKNESS =       .152E+00 M
FIRE HEIGHT =             0.0 M
FIRE DIAMETER =           2.0 M


LINK NO = 1     RADIUS =   2.0 M  DIST CEILING =   0.30 M
 RTI = 35.00 SQRT(MS)     FUSION TEMPERATURE FOR LINK =  352.16
LINK NO = 2     RADIUS =   4.0 M  DIST CEILING =   0.30 M
 RTI = 35.00 SQRT(MS)     FUSION TEMPERATURE FOR LINK =  352.16
LINK NO = 3     RADIUS =   6.0 M  DIST CEILING =   0.30 M
 RTI = 35.00 SQRT(MS)     FUSION TEMPERATURE FOR LINK =  352.16
LINK NO = 4     RADIUS =   8.0 M  DIST CEILING =   0.30 M
 RTI = 35.00 SQRT(MS)     FUSION TEMPERATURE FOR LINK =  352.16
VENT = 1   VENT AREA =   20.0 M2       LINK CONTROLLING VENT = 2
TIME (S)=   0.0000 LYR TEMP (K)=  293.2 LYR HT (M) =  10.00 LYR MASS
(KG)=0.000E+00
FIRE OUTPUT (W) = 0.0000E+00 VENT AREA (M2) =    0.00 PL TEMP (K)=   0.0 RAD
FRAC =   0.00
 LINK = 1 LINK TEMP (K) = 293.16 JET VELOCITY (M/S) =    0.000 JET TEMP (K) =
293.2
 LINK = 2 LINK TEMP (K) = 293.16 JET VELOCITY (M/S) =    0.000 JET TEMP (K) =
293.2
 LINK = 3 LINK TEMP (K) = 293.16 JET VELOCITY (M/S) =    0.000 JET TEMP (K) =
```

293.2
LINK = 4 LINK TEMP (K) = 293.16 JET VELOCITY (M/S) = 0.000 JET TEMP (K) = 293.2
R (M) = 0.00 TSL (K) = 293.2 QB (W/M2) = 0.000E+00 QT (W/M2) = 0.000E+00
R (M) = 3.03 TSL (K) = 293.2 QB (W/M2) = 0.000E+00 QT (W/M2) = 0.000E+00
R (M) = 6.06 TSL (K) = 293.2 QB (W/M2) = 0.000E+00 QT (W/M2) = 0.000E+00
R (M) = 9.08 TSL (K) = 293.2 QB (W/M2) = 0.000E+00 QT (W/M2) = 0.000E+00
R (M) = 12.11 TSL (K) = 293.2 QB (W/M2) = 0.000E+00 QT (W/M2) = 0.000E+00
R (M) = 15.14 TSL (K) = 293.2 QB (W/M2) = 0.000E+00 QT (W/M2) = 0.000E+00
TIME (S)= 25.0000 LYR TEMP (K)= 300.8 LYR HT (M) = 8.67 LYR MASS (KG)=0.470E+03
FIRE OUTPUT (W) = 0.6000E+06 VENT AREA (M2) = 0.00 PL TEMP (K)= 320.9 RAD FRAC = 0.45
LINK = 1 LINK TEMP (K) = 300.50 JET VELOCITY (M/S) = 1.951 JET TEMP (K) = 314.5
LINK = 2 LINK TEMP (K) = 297.56 JET VELOCITY (M/S) = 1.095 JET TEMP (K) = 309.9
LINK = 3 LINK TEMP (K) = 296.39 JET VELOCITY (M/S) = 0.781 JET TEMP (K) = 307.8
LINK = 4 LINK TEMP (K) = 295.75 JET VELOCITY (M/S) = 0.615 JET TEMP (K) = 306.4
R (M) = 0.00 TSL (K) = 298.1 QB (W/M2) = 0.476E+03 QT (W/M2) = 0.195E-11
R (M) = 3.03 TSL (K) = 296.5 QB (W/M2) = 0.332E+03 QT (W/M2) = 0.195E-11
R (M) = 6.06 TSL (K) = 295.2 QB (W/M2) = 0.210E+03 QT (W/M2) = 0.195E-11
R (M) = 9.08 TSL (K) = 294.5 QB (W/M2) = 0.135E+03 QT (W/M2) = 0.195E-11
R (M) = 12.11 TSL (K) = 294.0 QB (W/M2) = 0.907E+02 QT (W/M2) = 0.195E-11
R (M) = 15.14 TSL (K) = 293.5 QB (W/M2) = 0.341E+02 QT (W/M2) = 0.195E-11
TIME (S)= 50.0000 LYR TEMP (K)= 307.4 LYR HT (M) = 7.03 LYR MASS (KG)=0.102E+04
FIRE OUTPUT (W) = 0.1200E+07 VENT AREA (M2) = 0.00 PL TEMP (K)= 341.1 RAD FRAC = 0.45
LINK = 1 LINK TEMP (K) = 313.10 JET VELOCITY (M/S) = 2.298 JET TEMP (K) = 332.0
LINK = 2 LINK TEMP (K) = 306.90 JET VELOCITY (M/S) = 1.290 JET TEMP (K) = 325.8
LINK = 3 LINK TEMP (K) = 304.07 JET VELOCITY (M/S) = 0.920 JET TEMP (K) = 322.6
LINK = 4 LINK TEMP (K) = 302.37 JET VELOCITY (M/S) = 0.724 JET TEMP (K) = 320.5
R (M) = 0.00 TSL (K) = 307.3 QB (W/M2) = 0.825E+03 QT (W/M2) = 0.227E-11
R (M) = 3.03 TSL (K) = 303.2 QB (W/M2) = 0.604E+03 QT (W/M2) = 0.227E-11
R (M) = 6.06 TSL (K) = 299.6 QB (W/M2) = 0.395E+03 QT (W/M2) = 0.227E-11
R (M) = 9.08 TSL (K) = 297.3 QB (W/M2) = 0.259E+03 QT (W/M2) = 0.227E-11

R (M) = 12.11 TSL (K) = 296.0 QB (W/M2) = 0.177E+03 QT (W/M2) = 0.227E-11
R (M) = 15.14 TSL (K) = 294.2 QB (W/M2) = 0.660E+02 QT (W/M2) = 0.227E-11
TIME (S)= 75.0000 LYR TEMP (K)= 315.8 LYR HT (M) = 6.31 LYR MASS
(KG)=0.124E+04
FIRE OUTPUT (W) = 0.1800E+07 VENT AREA (M2) = 0.00 PL TEMP (K)= 363.7 RAD
FRAC = 0.40
LINK = 1 LINK TEMP (K) = 327.46 JET VELOCITY (M/S) = 2.685 JET TEMP (K) =
350.6
LINK = 2 LINK TEMP (K) = 318.19 JET VELOCITY (M/S) = 1.507 JET TEMP (K) =
341.8
LINK = 3 LINK TEMP (K) = 313.71 JET VELOCITY (M/S) = 1.075 JET TEMP (K) =
337.2
LINK = 4 LINK TEMP (K) = 310.93 JET VELOCITY (M/S) = 0.846 JET TEMP (K) =
334.3
R (M) = 0.00 TSL (K) = 318.3 QB (W/M2) = 0.111E+04 QT (W/M2) = 0.195E-11
R (M) = 3.03 TSL (K) = 311.5 QB (W/M2) = 0.823E+03 QT (W/M2) = 0.195E-11
R (M) = 6.06 TSL (K) = 305.1 QB (W/M2) = 0.546E+03 QT (W/M2) = 0.195E-11
R (M) = 9.08 TSL (K) = 301.0 QB (W/M2) = 0.363E+03 QT (W/M2) = 0.195E-11
R (M) = 12.11 TSL (K) = 298.5 QB (W/M2) = 0.253E+03 QT (W/M2) = 0.195E-11
R (M) = 15.14 TSL (K) = 295.1 QB (W/M2) = 0.849E+02 QT (W/M2) = 0.195E-11
TIME (S)= 100.0000 LYR TEMP (K)= 327.2 LYR HT (M) = 6.31 LYR MASS
(KG)=0.120E+04
FIRE OUTPUT (W) = 0.2400E+07 VENT AREA (M2) = 0.00 PL TEMP (K)= 386.6 RAD
FRAC = 0.35
LINK = 1 LINK TEMP (K) = 342.62 JET VELOCITY (M/S) = 3.035 JET TEMP (K) =
369.3
LINK = 2 LINK TEMP (K) = 330.20 JET VELOCITY (M/S) = 1.704 JET TEMP (K) =
357.6
LINK = 3 LINK TEMP (K) = 324.07 JET VELOCITY (M/S) = 1.215 JET TEMP (K) =
351.6
LINK = 4 LINK TEMP (K) = 320.20 JET VELOCITY (M/S) = 0.956 JET TEMP (K) =
347.7
R (M) = 0.00 TSL (K) = 329.8 QB (W/M2) = 0.133E+04 QT (W/M2) = 0.227E-11
R (M) = 3.03 TSL (K) = 320.2 QB (W/M2) = 0.100E+04 QT (W/M2) = 0.227E-11
R (M) = 6.06 TSL (K) = 311.0 QB (W/M2) = 0.673E+03 QT (W/M2) = 0.227E-11
R (M) = 9.08 TSL (K) = 305.1 QB (W/M2) = 0.457E+03 QT (W/M2) = 0.227E-11
R (M) = 12.11 TSL (K) = 301.5 QB (W/M2) = 0.325E+03 QT (W/M2) = 0.227E-11
R (M) = 15.14 TSL (K) = 295.9 QB (W/M2) = 0.961E+02 QT (W/M2) = 0.227E-11
TIME (S)= 125.0000 LYR TEMP (K)= 338.9 LYR HT (M) = 6.34 LYR MASS
(KG)=0.114E+04
FIRE OUTPUT (W) = 0.2700E+07 VENT AREA (M2) = 0.00 PL TEMP (K)= 400.4 RAD
FRAC = 0.34
LINK = 1 LINK TEMP (K) = 355.02 JET VELOCITY (M/S) = 3.178 JET TEMP (K) =

380.5

LINK = 2 LINK TEMP (K) = 340.35 JET VELOCITY (M/S) =   1.784 JET TEMP (K) = 367.1

LINK = 3 LINK TEMP (K) = 333.00 JET VELOCITY (M/S) =   1.272 JET TEMP (K) = 360.2

LINK = 4 LINK TEMP (K) = 328.30 JET VELOCITY (M/S) =   1.001 JET TEMP (K) = 355.7

TIME LINK   1 OPENS EQUALS   118.6676 (S)

R (M) =   0.00 TSL (K) =   339.7 QB (W/M2) = 0.135E+04 QT (W/M2) = 0.227E-11
R (M) =   3.03 TSL (K) =   328.0 QB (W/M2) = 0.104E+04 QT (W/M2) = 0.227E-11
R (M) =   6.06 TSL (K) =   316.6 QB (W/M2) = 0.724E+03 QT (W/M2) = 0.227E-11
R (M) =   9.08 TSL (K) =   309.1 QB (W/M2) = 0.505E+03 QT (W/M2) = 0.227E-11
R (M) =   12.11 TSL (K) =   304.4 QB (W/M2) = 0.366E+03 QT (W/M2) = 0.227E-11
R (M) =   15.14 TSL (K) =   296.6 QB (W/M2) = 0.101E+03 QT (W/M2) = 0.227E-11

TIME (S)= 150.0000 LYR TEMP (K)= 348.9 LYR HT (M) =   6.37 LYR MASS (KG)=0.110E+04

FIRE OUTPUT (W) = 0.3000E+07 VENT AREA (M2) =   0.00 PL TEMP (K)= 413.1 RAD FRAC =   0.32

LINK = 1 LINK TEMP (K) = 364.48 JET VELOCITY (M/S) =   3.313 JET TEMP (K) = 390.9

LINK = 2 LINK TEMP (K) = 348.18 JET VELOCITY (M/S) =   1.859 JET TEMP (K) = 375.8

LINK = 3 LINK TEMP (K) = 339.96 JET VELOCITY (M/S) =   1.326 JET TEMP (K) = 368.1

LINK = 4 LINK TEMP (K) = 334.68 JET VELOCITY (M/S) =   1.043 JET TEMP (K) = 363.1

TIME LINK   1 OPENS EQUALS   118.6676 (S)

R (M) =   0.00 TSL (K) =   347.9 QB (W/M2) = 0.138E+04 QT (W/M2) = 0.227E-11
R (M) =   3.03 TSL (K) =   334.8 QB (W/M2) = 0.108E+04 QT (W/M2) = 0.227E-11
R (M) =   6.06 TSL (K) =   321.7 QB (W/M2) = 0.769E+03 QT (W/M2) = 0.227E-11
R (M) =   9.08 TSL (K) =   312.8 QB (W/M2) = 0.544E+03 QT (W/M2) = 0.227E-11
R (M) =   12.11 TSL (K) =   307.2 QB (W/M2) = 0.399E+03 QT (W/M2) = 0.227E-11
R (M) =   15.14 TSL (K) =   297.3 QB (W/M2) = 0.106E+03 QT (W/M2) = 0.227E-11

TIME (S)= 175.0000 LYR TEMP (K)= 356.3 LYR HT (M) =   7.25 LYR MASS (KG)=0.817E+03

FIRE OUTPUT (W) = 0.3300E+07 VENT AREA (M2) =   20.00 PL TEMP (K)= 416.1 RAD FRAC =   0.31

LINK = 1 LINK TEMP (K) = 370.88 JET VELOCITY (M/S) =   3.483 JET TEMP (K) = 392.4

LINK = 2 LINK TEMP (K) = 353.54 JET VELOCITY (M/S) =   1.955 JET TEMP (K) = 376.1

LINK = 3 LINK TEMP (K) = 344.77 JET VELOCITY (M/S) =   1.394 JET TEMP (K) = 367.9

LINK = 4 LINK TEMP (K) = 339.12 JET VELOCITY (M/S) = 1.097 JET TEMP (K) = 362.5
TIME LINK 1 OPENS EQUALS 118.6676 (S)
TIME LINK 2 OPENS EQUALS 164.1054 (S)
R (M) = 0.00 TSL (K) = 354.7 QB (W/M2) = 0.129E+04 QT (W/M2) = 0.227E-11
R (M) = 3.03 TSL (K) = 340.4 QB (W/M2) = 0.103E+04 QT (W/M2) = 0.227E-11
R (M) = 6.06 TSL (K) = 326.1 QB (W/M2) = 0.749E+03 QT (W/M2) = 0.227E-11
R (M) = 9.08 TSL (K) = 316.1 QB (W/M2) = 0.538E+03 QT (W/M2) = 0.227E-11
R (M) = 12.11 TSL (K) = 309.7 QB (W/M2) = 0.398E+03 QT (W/M2) = 0.227E-11
R (M) = 15.14 TSL (K) = 297.9 QB (W/M2) = 0.110E+03 QT (W/M2) = 0.227E-11
TIME (S)= 200.0000 LYR TEMP (K)= 356.8 LYR HT (M) = 7.95 LYR MASS (KG)=0.609E+03
FIRE OUTPUT (W) = 0.3600E+07 VENT AREA (M2) = 20.00 PL TEMP (K)= 416.3
RAD FRAC = 0.30
LINK = 1 LINK TEMP (K) = 370.94 JET VELOCITY (M/S) = 3.684 JET TEMP (K) = 391.0
LINK = 2 LINK TEMP (K) = 353.62 JET VELOCITY (M/S) = 2.067 JET TEMP (K) = 373.4
LINK = 3 LINK TEMP (K) = 344.88 JET VELOCITY (M/S) = 1.475 JET TEMP (K) = 364.6
LINK = 4 LINK TEMP (K) = 339.24 JET VELOCITY (M/S) = 1.160 JET TEMP (K) = 359.0
TIME LINK 1 OPENS EQUALS 118.6676 (S)
TIME LINK 2 OPENS EQUALS 164.1054 (S)
R (M) = 0.00 TSL (K) = 359.0 QB (W/M2) = 0.125E+04 QT (W/M2) = 0.584E-11
R (M) = 3.03 TSL (K) = 344.2 QB (W/M2) = 0.993E+03 QT (W/M2) = 0.584E-11
R (M) = 6.06 TSL (K) = 329.1 QB (W/M2) = 0.725E+03 QT (W/M2) = 0.584E-11
R (M) = 9.08 TSL (K) = 318.4 QB (W/M2) = 0.523E+03 QT (W/M2) = 0.584E-11
R (M) = 12.11 TSL (K) = 311.5 QB (W/M2) = 0.387E+03 QT (W/M2) = 0.584E-11
R (M) = 15.14 TSL (K) = 298.5 QB (W/M2) = 0.113E+03 QT (W/M2) = 0.584E-11
TIME (S)= 225.0000 LYR TEMP (K)= 358.4 LYR HT (M) = 8.09 LYR MASS (KG)=0.565E+03
FIRE OUTPUT (W) = 0.3900E+07 VENT AREA (M2) = 20.00 PL TEMP (K)= 422.4
RAD FRAC = 0.29
LINK = 1 LINK TEMP (K) = 372.64 JET VELOCITY (M/S) = 3.829 JET TEMP (K) = 395.4
LINK = 2 LINK TEMP (K) = 354.09 JET VELOCITY (M/S) = 2.149 JET TEMP (K) = 376.5
LINK = 3 LINK TEMP (K) = 345.05 JET VELOCITY (M/S) = 1.533 JET TEMP (K) = 367.1
LINK = 4 LINK TEMP (K) = 339.32 JET VELOCITY (M/S) = 1.206 JET TEMP (K) = 361.1
TIME LINK 1 OPENS EQUALS 118.6676 (S)

TIME LINK 2 OPENS EQUALS   164.1054 (S)
R (M) =   0.00 TSL (K) =   363.7 QB (W/M2) = 0.129E+04 QT (W/M2) = 0.101E-10
R (M) =   3.03 TSL (K) =   348.0 QB (W/M2) = 0.102E+04 QT (W/M2) = 0.101E-10
R (M) =   6.06 TSL (K) =   332.0 QB (W/M2) = 0.741E+03 QT (W/M2) = 0.101E-10
R (M) =   9.08 TSL (K) =   320.6 QB (W/M2) = 0.535E+03 QT (W/M2) = 0.101E-10
R (M) =   12.11 TSL (K) =   313.2 QB (W/M2) = 0.397E+03 QT (W/M2) = 0.101E-10
R (M) =   15.14 TSL (K) =   299.0 QB (W/M2) = 0.115E+03 QT (W/M2) = 0.101E-10
TIME (S)= 250.0000 LYR TEMP (K)=   362.2 LYR HT (M) =   8.10 LYR MASS
(KG)=0.557E+03
FIRE OUTPUT (W) =   0.4200E+07 VENT AREA (M2) =   20.00 PL TEMP (K)=   430.5
RAD FRAC =   0.28
 LINK = 1 LINK TEMP (K) =   377.04 JET VELOCITY (M/S) =   3.949 JET TEMP (K) =
401.7
 LINK = 2 LINK TEMP (K) =   356.88 JET VELOCITY (M/S) =   2.216 JET TEMP (K) =
381.7
 LINK = 3 LINK TEMP (K) =   347.08 JET VELOCITY (M/S) =   1.581 JET TEMP (K) =
371.7
 LINK = 4 LINK TEMP (K) =   340.91 JET VELOCITY (M/S) =   1.244 JET TEMP (K) =
365.3
TIME LINK   1 OPENS EQUALS   118.6676 (S)
TIME LINK   2 OPENS EQUALS   164.1054 (S)
R (M) =   0.00 TSL (K) =   368.9 QB (W/M2) = 0.133E+04 QT (W/M2) = 0.114E-10
R (M) =   3.03 TSL (K) =   352.2 QB (W/M2) = 0.105E+04 QT (W/M2) = 0.114E-10
R (M) =   6.06 TSL (K) =   335.2 QB (W/M2) = 0.765E+03 QT (W/M2) = 0.114E-10
R (M) =   9.08 TSL (K) =   323.0 QB (W/M2) = 0.554E+03 QT (W/M2) = 0.114E-10
R (M) =   12.11 TSL (K) =   315.0 QB (W/M2) = 0.414E+03 QT (W/M2) = 0.114E-10
R (M) =   15.14 TSL (K) =   299.5 QB (W/M2) = 0.117E+03 QT (W/M2) = 0.114E-10
TIME (S)= 275.0000 LYR TEMP (K)=   366.9 LYR HT (M) =   8.09 LYR MASS
(KG)=0.552E+03
FIRE OUTPUT (W) =   0.4500E+07 VENT AREA (M2) =   20.00 PL TEMP (K)=   439.0
RAD FRAC =   0.26
 LINK = 1 LINK TEMP (K) =   382.46 JET VELOCITY (M/S) =   4.062 JET TEMP (K) =
408.5
 LINK = 2 LINK TEMP (K) =   360.86 JET VELOCITY (M/S) =   2.280 JET TEMP (K) =
387.2
 LINK = 3 LINK TEMP (K) =   350.33 JET VELOCITY (M/S) =   1.626 JET TEMP (K) =
376.6
 LINK = 4 LINK TEMP (K) =   343.70 JET VELOCITY (M/S) =   1.279 JET TEMP (K) =
369.9
TIME LINK   1 OPENS EQUALS   118.6676 (S)
TIME LINK   2 OPENS EQUALS   164.1054 (S)
R (M) =   0.00 TSL (K) =   374.2 QB (W/M2) = 0.136E+04 QT (W/M2) = 0.136E-10
R (M) =   3.03 TSL (K) =   356.4 QB (W/M2) = 0.108E+04 QT (W/M2) = 0.136E-10

R (M) = 6.06 TSL (K) = 338.3 QB (W/M2) = 0.786E+03 QT (W/M2) = 0.136E-10
R (M) = 9.08 TSL (K) = 325.4 QB (W/M2) = 0.572E+03 QT (W/M2) = 0.136E-10
R (M) = 12.11 TSL (K) = 316.9 QB (W/M2) = 0.430E+03 QT (W/M2) = 0.136E-10
R (M) = 15.14 TSL (K) = 300.0 QB (W/M2) = 0.117E+03 QT (W/M2) = 0.136E-10
TIME (S)= 300.0000 LYR TEMP (K)= 371.7 LYR HT (M) = 8.08 LYR MASS (KG)=0.548E+03
FIRE OUTPUT (W) = 0.4800E+07 VENT AREA (M2) = 20.00 PL TEMP (K)= 447.7 RAD FRAC = 0.25
LINK = 1 LINK TEMP (K) = 388.18 JET VELOCITY (M/S) = 4.172 JET TEMP (K) = 415.4
LINK = 2 LINK TEMP (K) = 365.24 JET VELOCITY (M/S) = 2.341 JET TEMP (K) = 392.9
LINK = 3 LINK TEMP (K) = 354.02 JET VELOCITY (M/S) = 1.670 JET TEMP (K) = 381.7
LINK = 4 LINK TEMP (K) = 346.94 JET VELOCITY (M/S) = 1.314 JET TEMP (K) = 374.5
TIME LINK 1 OPENS EQUALS 118.6676 (S)
TIME LINK 2 OPENS EQUALS 164.1054 (S)
TIME LINK 3 OPENS EQUALS 288.0000 (S)
R (M) = 0.00 TSL (K) = 379.4 QB (W/M2) = 0.138E+04 QT (W/M2) = 0.178E-10
R (M) = 3.03 TSL (K) = 360.6 QB (W/M2) = 0.110E+04 QT (W/M2) = 0.178E-10
R (M) = 6.06 TSL (K) = 341.5 QB (W/M2) = 0.804E+03 QT (W/M2) = 0.178E-10
R (M) = 9.08 TSL (K) = 327.8 QB (W/M2) = 0.589E+03 QT (W/M2) = 0.178E-10
R (M) = 12.11 TSL (K) = 318.7 QB (W/M2) = 0.444E+03 QT (W/M2) = 0.178E-10
R (M) = 15.14 TSL (K) = 300.4 QB (W/M2) = 0.117E+03 QT (W/M2) = 0.178E-10
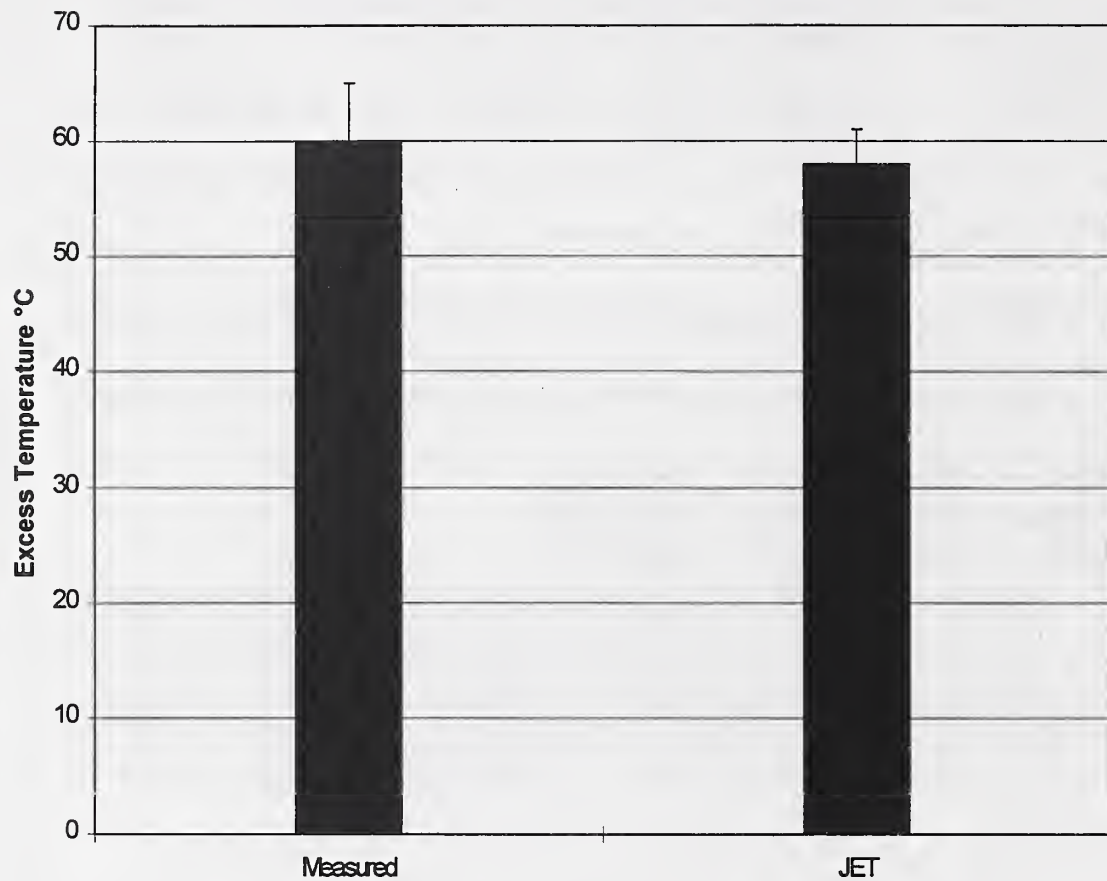
Figure 1 Comparison of measured and predicted plume centerline temperature for the 0.58 m high ceiling experiment. The experimental uncertainty interval was given in the reference while the predicted uncertainty interval was calculated assuming a ± 5 % uncertainty in the HRR.
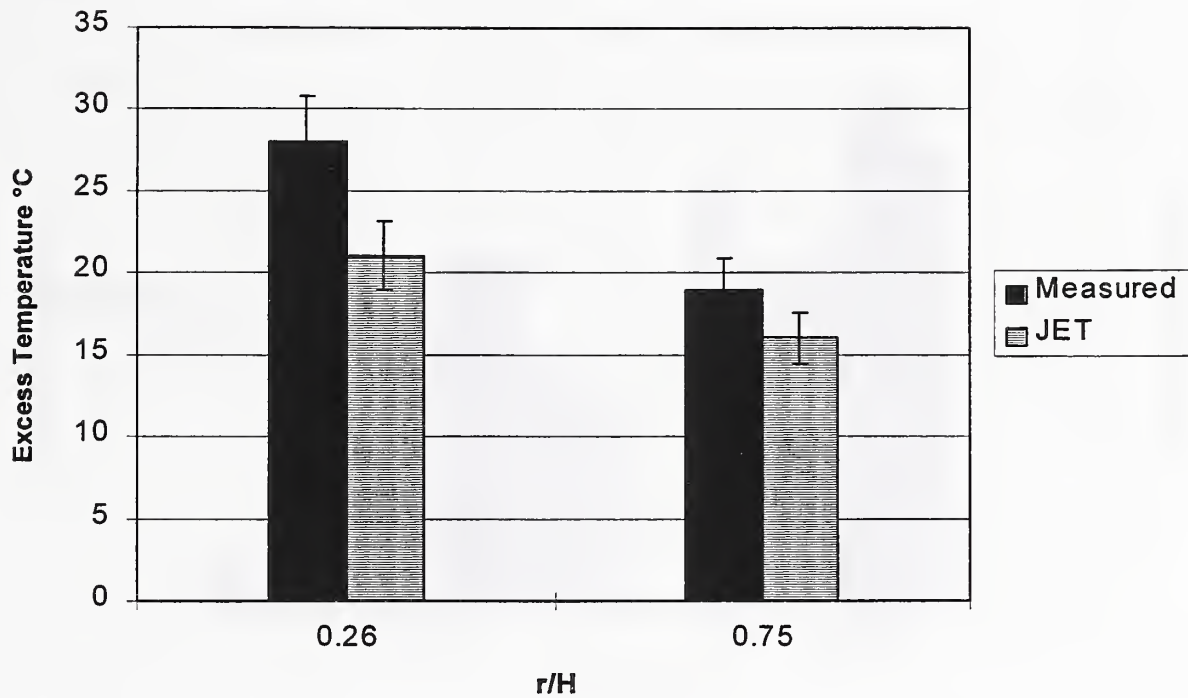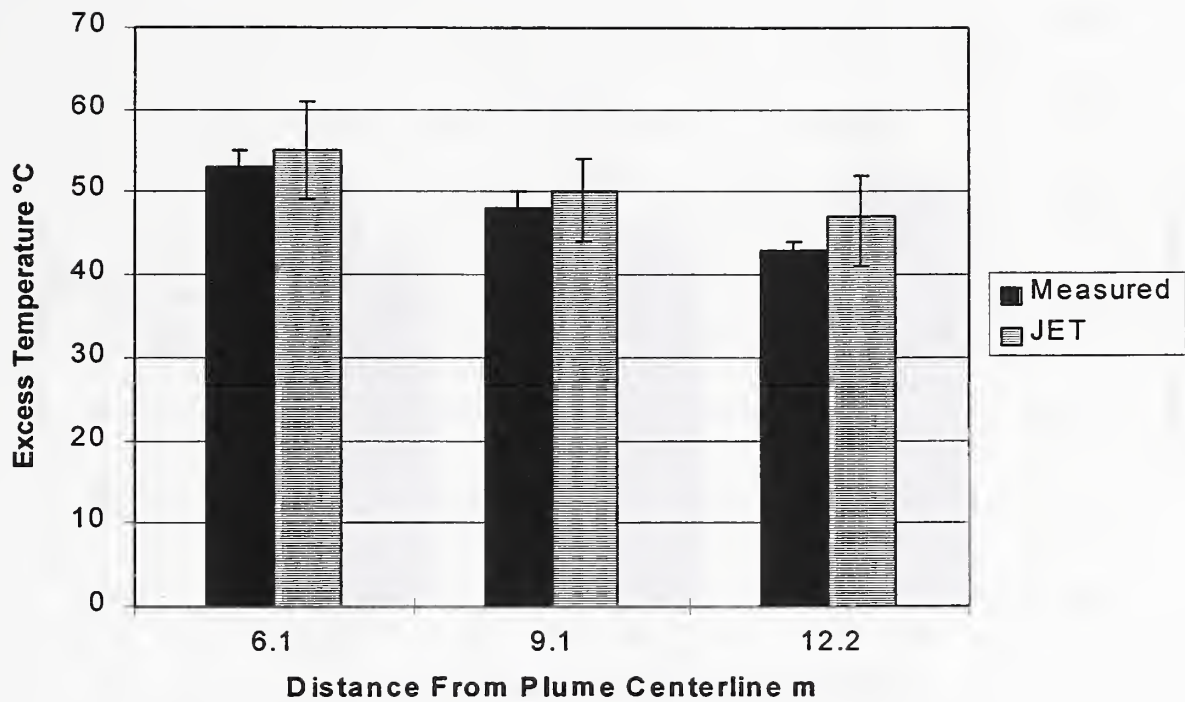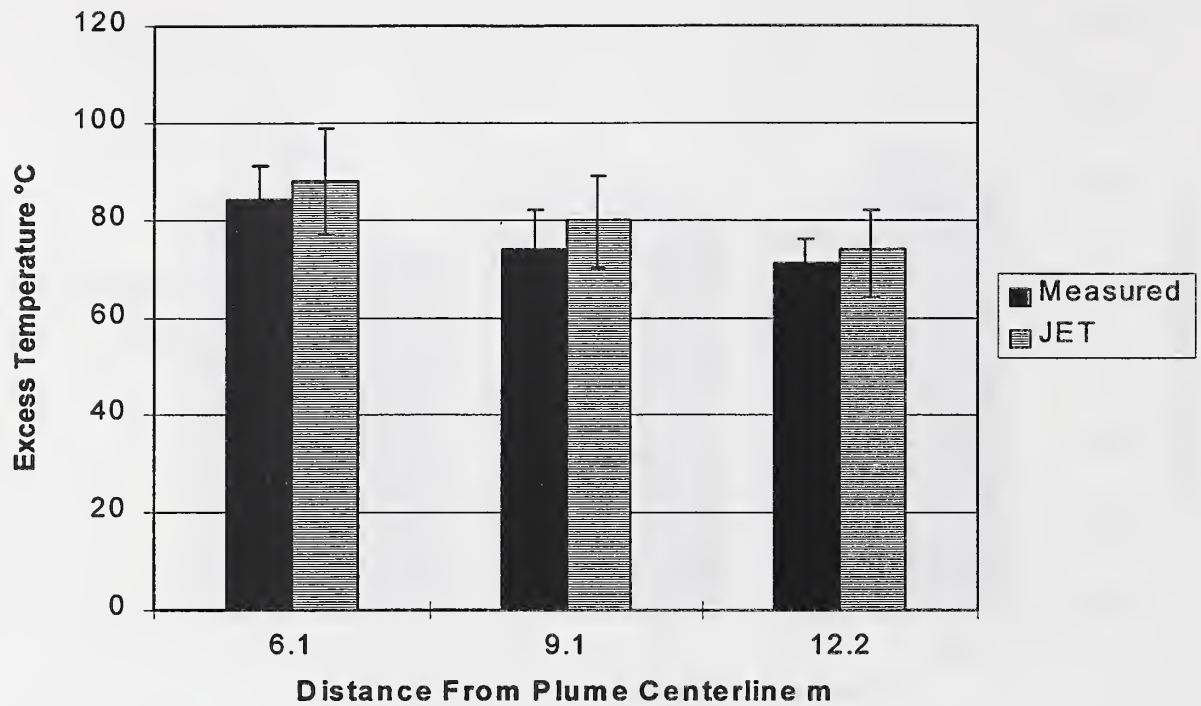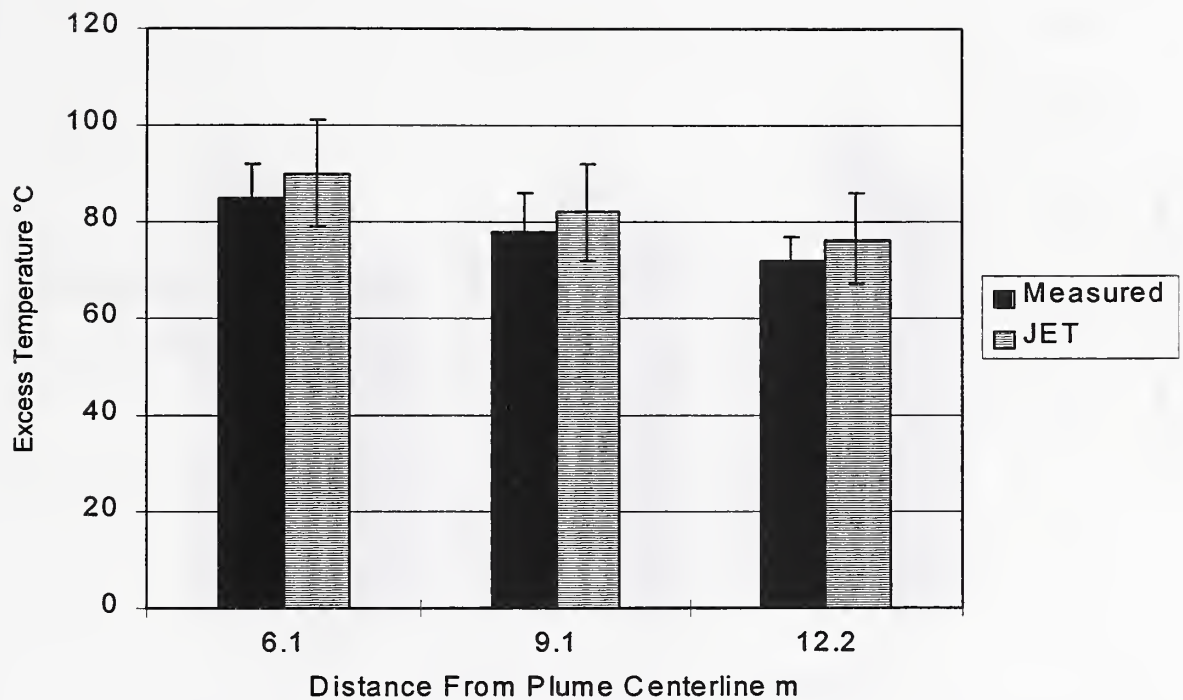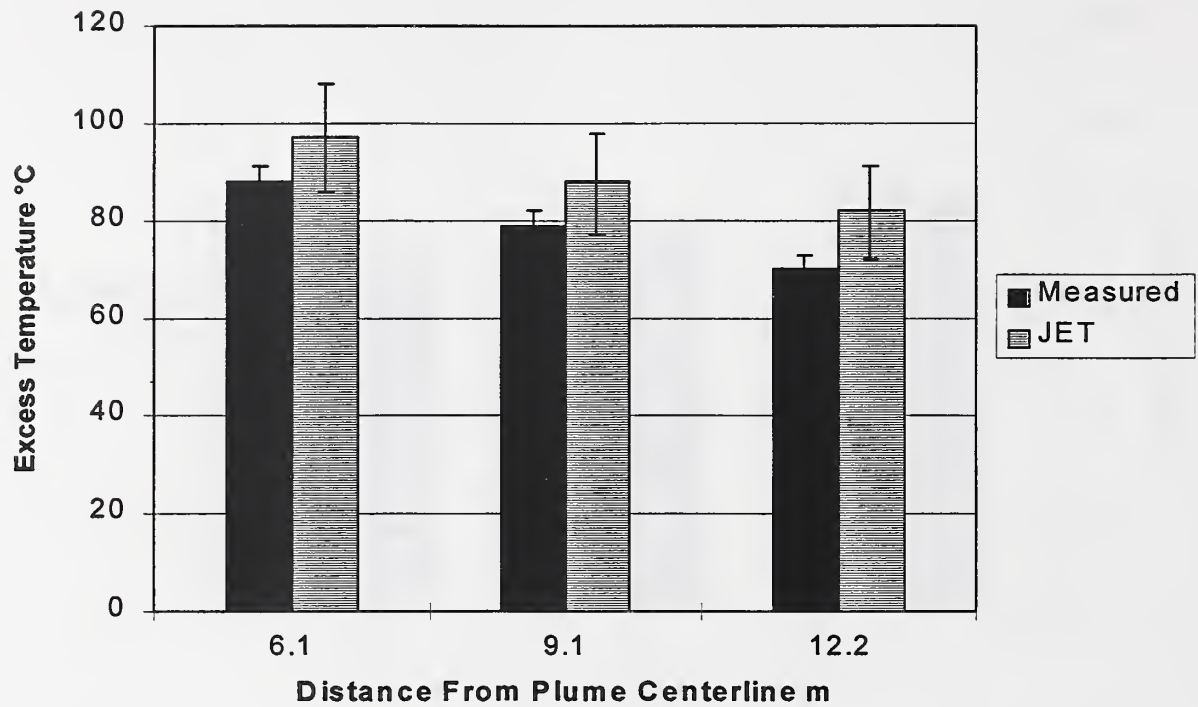
Figure 2 Comparison of measured and predicted ceiling jet temperature for the 1.0 m high ceiling experiment with a 0.75 kW HRR. A ± 10 % uncertainty interval was used for both the measurements and predictions.
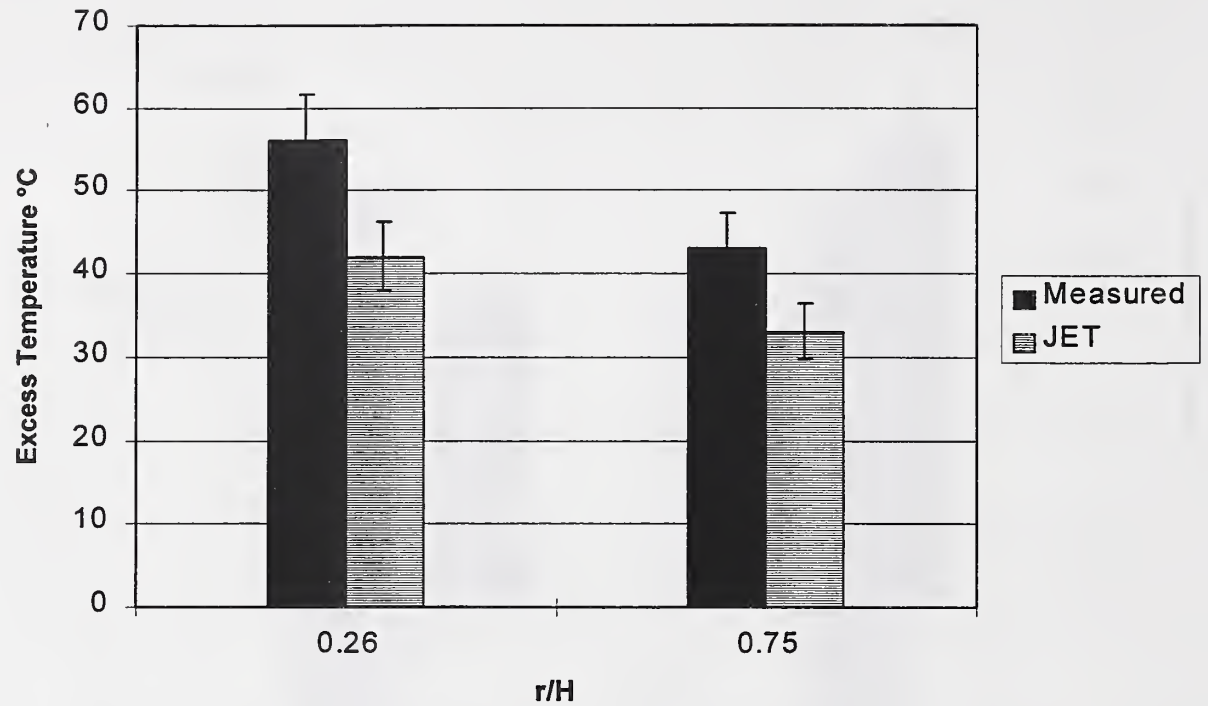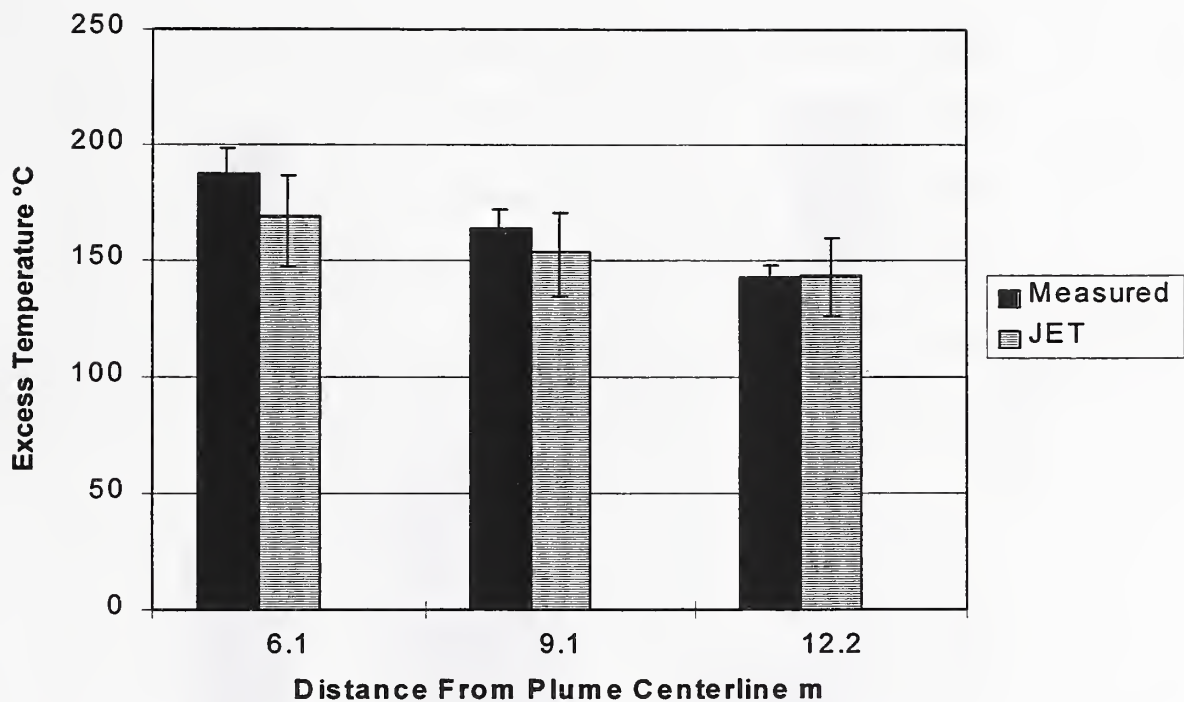
Figure 3 Comparison of measured and predicted ceiling jet temperature for the 1.0 m high ceiling experiment with a 2.0 kW HRR. A ± 10 % uncertainty interval was used for both the measurements and the predictions.
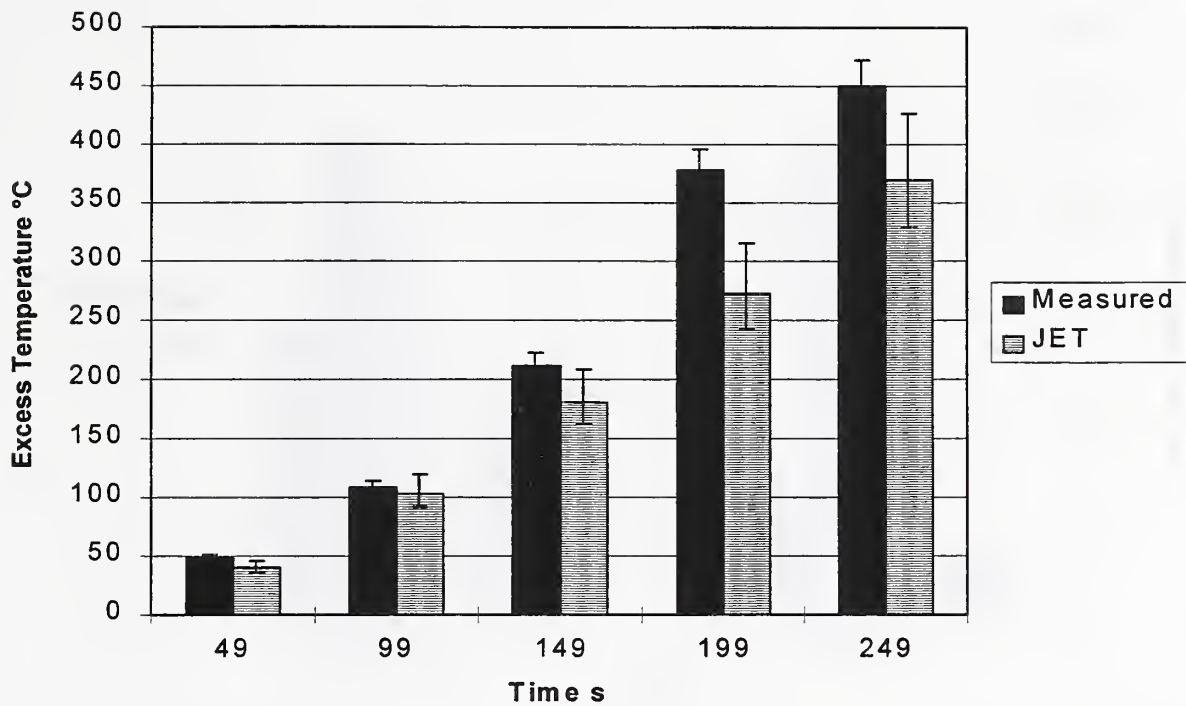
Figure 4 Comparison of measured and predicted plume centerline temperature for the 2.7 m high ceiling experiment without draft curtains. The uncertainty intervals for the data are ± 5 % while the uncertainty intervals for the predictions are based on varying the radiative fraction between 0.2 and 0.45. The predictions shown in the figure are calculated using a radiative fraction of 0.35.
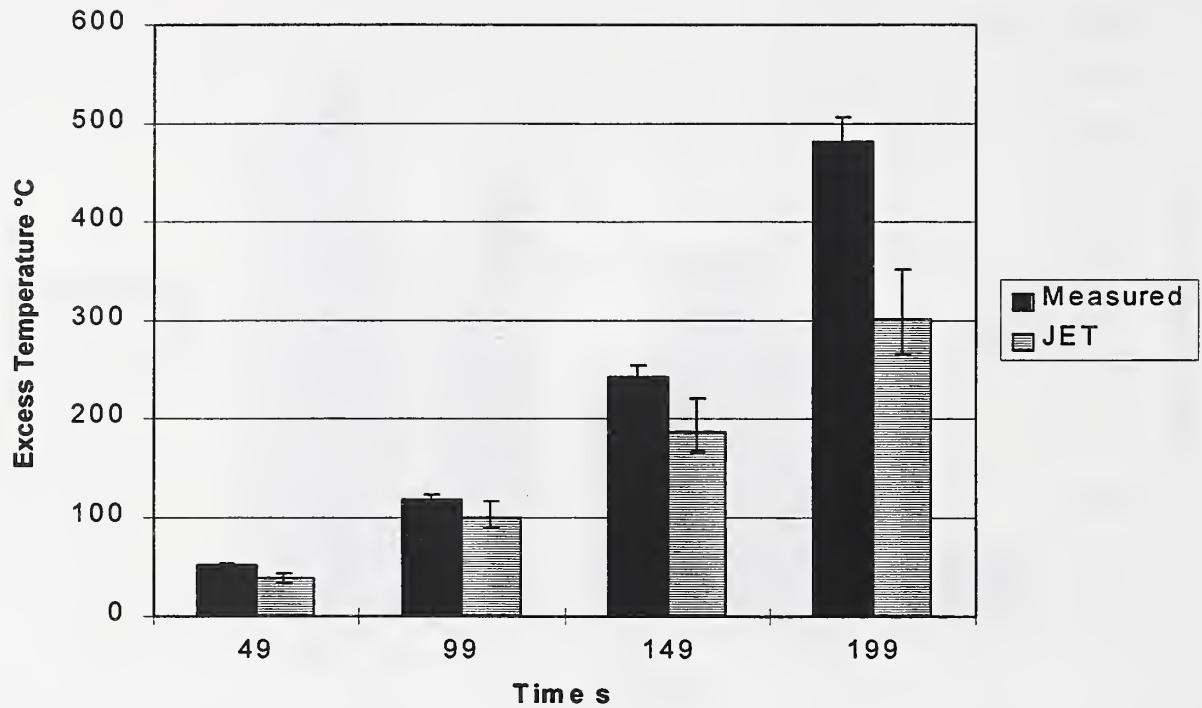
Figure 5 Comparison of measured and predicted plume centerline temperature for the 2.7 m high ceiling experiment with draft curtains. The uncertainty intervals for the data are ± 5 % while the uncertainty intervals for the predictions are based on varying the radiative fraction between 0.2 and 0.45. The predictions shown in the figure are calculated using a radiative fraction of 0.35.
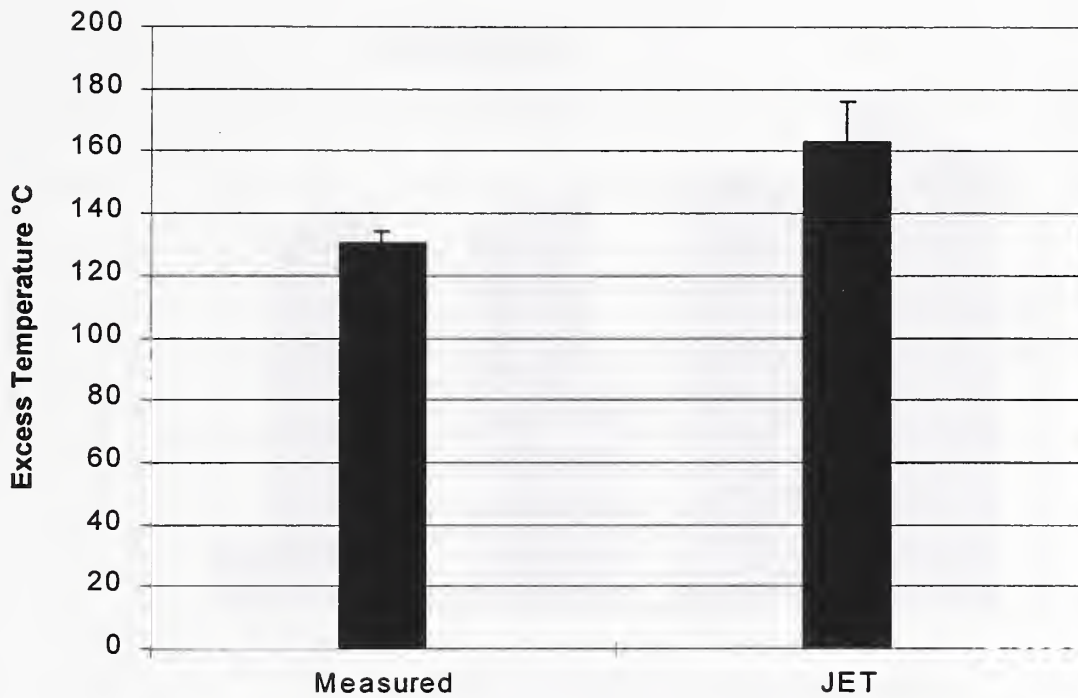
Figure 6 Comparison of measured and predicted plume centerline temperature for the 10 m high ceiling experiment. The uncertainty interval for the measurement is ± 4 °C while the uncertainty in the prediction is based on varying the radiative fraction between 0.25 and 0.40 with the predictions shown in the figure based on a radiative fraction of 0.34.
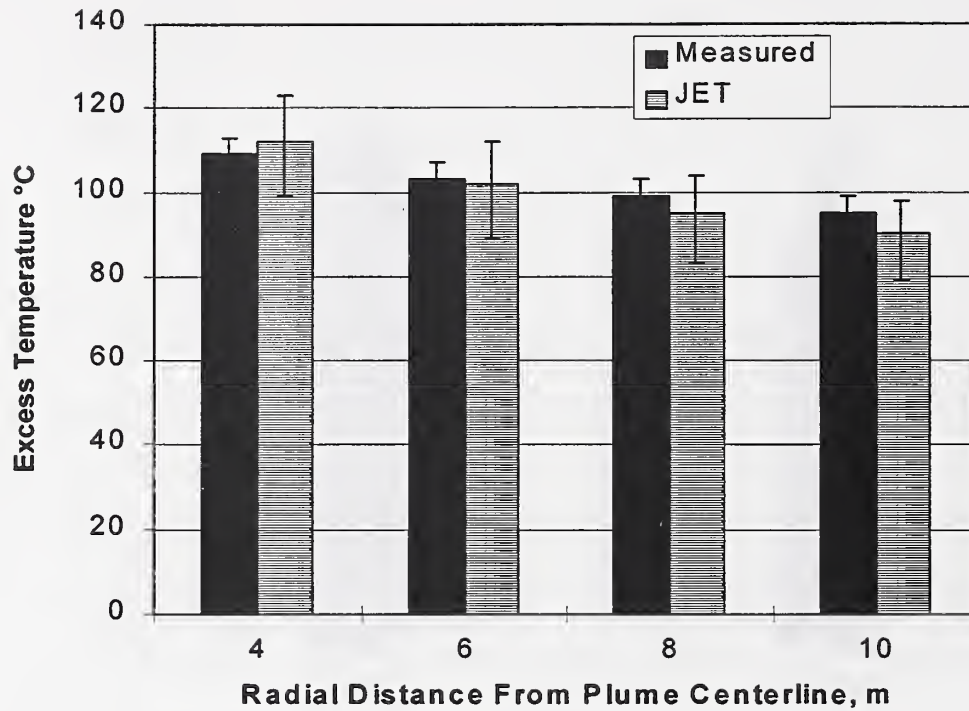
Figure 7 Comparison of measured and predicted ceiling jet temperature for the 10 m high ceiling experiment. The uncertainty interval for the measurement is ± 4 °C while the uncertainty in the prediction is based on varying the radiative fraction between 0.25 and 0.40 with the predictions shown in the figure based on a radiative fraction of 0.34.
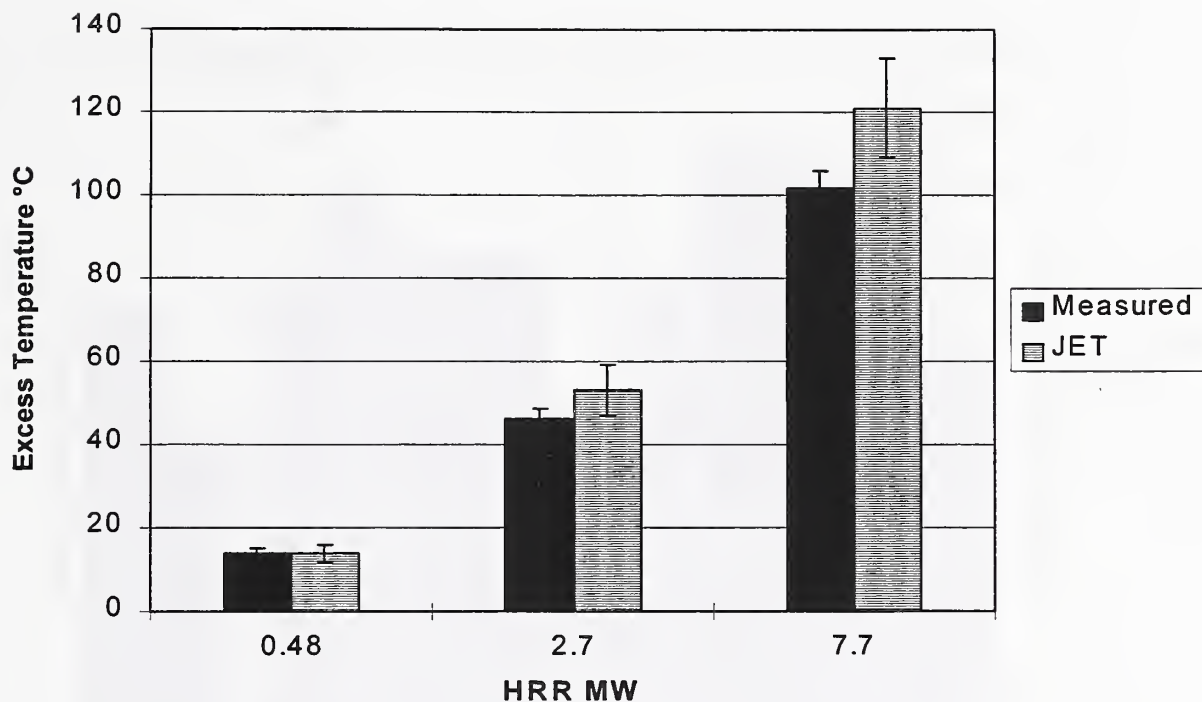
Figure 8 Comparison of measured and predicted plume centerline temperature for the 15 m high ceiling experiment. The uncertainty interval for the measurements is based on the measured RMS temperature fluctuation and is equal to $\pm \sigma$. The uncertainty in the prediction is based on varying the radiative fraction by $\pm 15 \%$.
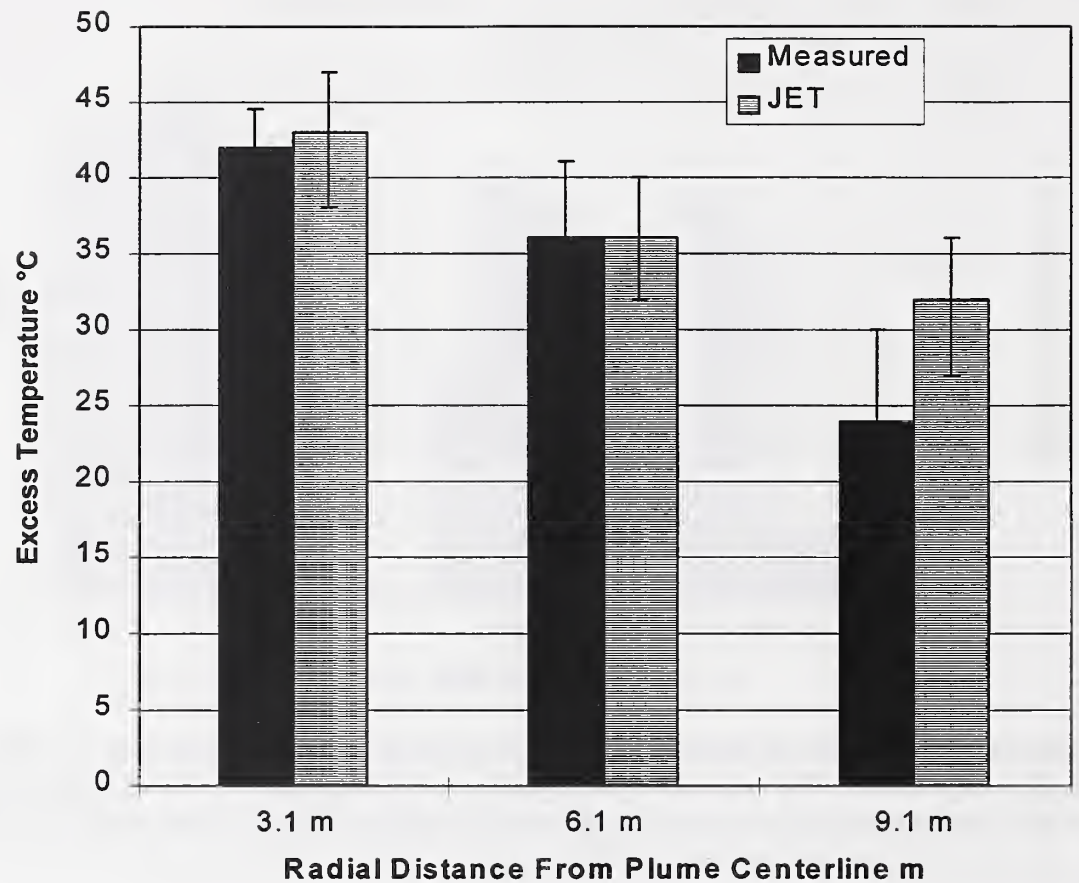
Figure 9 Comparison of measured and predicted ceiling jet temperature for the 15 m high ceiling experiment with a HRR of 2.8 MW. The uncertainty interval for the measurements is based on the measured RMS temperature fluctuation and is equal to ± σ. The uncertainty in the predictions is based on varying the radiative fraction by ± 15 %.
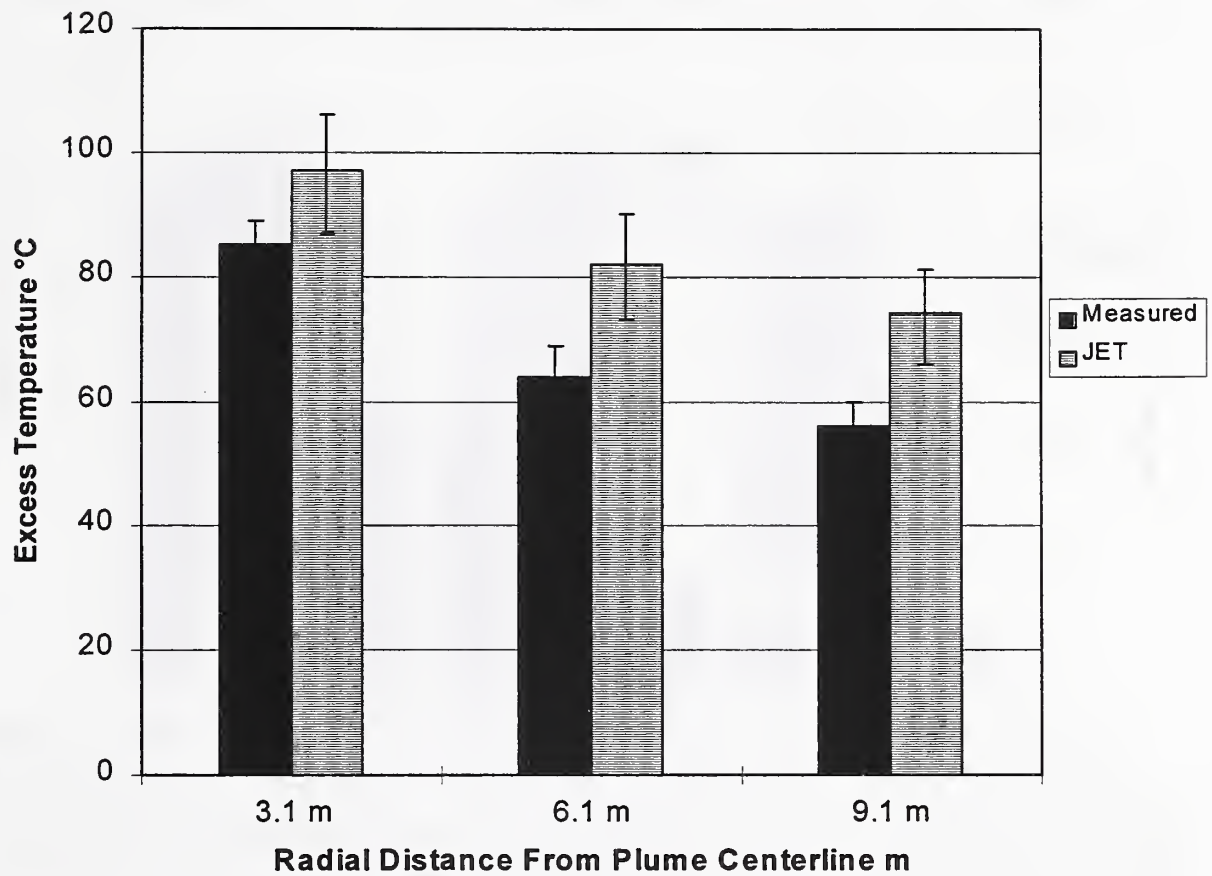
Figure 10 Comparison of measured and predicted ceiling jet temperature for the 15 m high ceiling experiment with a HRR of 7.7 MW. The uncertainty interval for the measurements is based on the measure RMS temperature fluctuation and is equal to ± σ. The uncertainty in the predictions is based on varying the radiative fraction by ± 15 %.
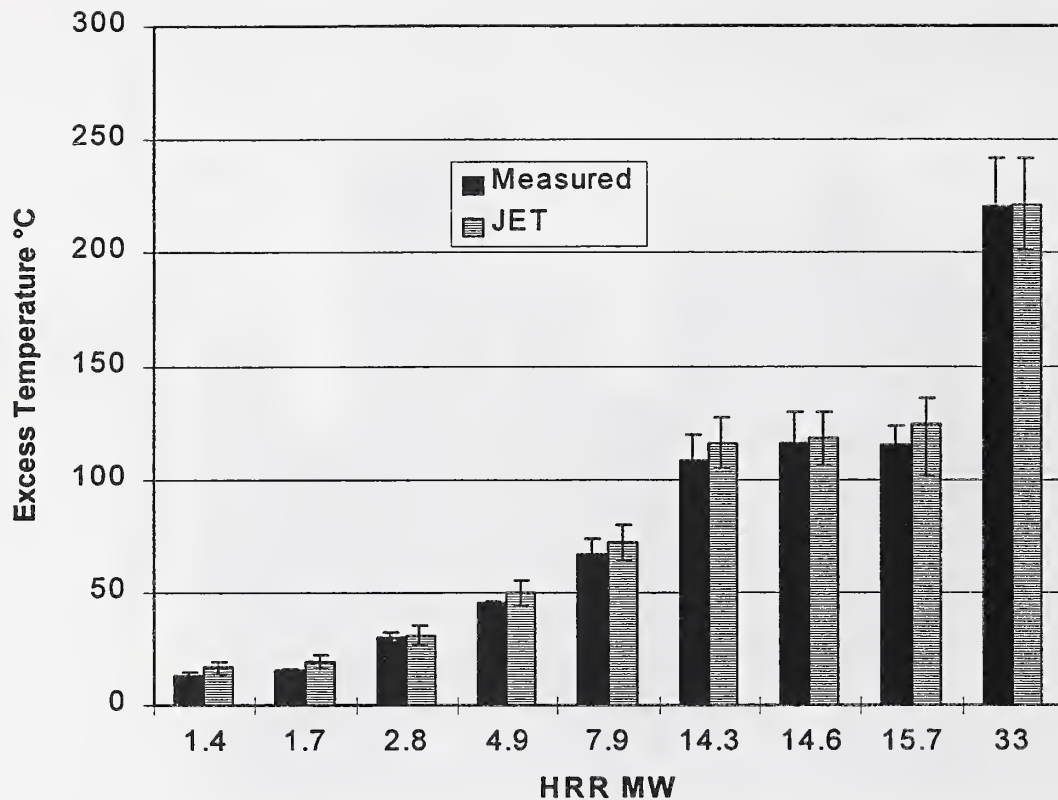
Figure 11 Comparison of measured and predicted plume centerline temperature for the 22 m high ceiling experiments. The HRR for each experiment is shown on the x axis. Uncertainty in measured temperature is based on the measured RMS temperature fluctuation and is equal to ± σ. The uncertainty in the predictions is estimated by varying the radiative fraction by ± 15 %.
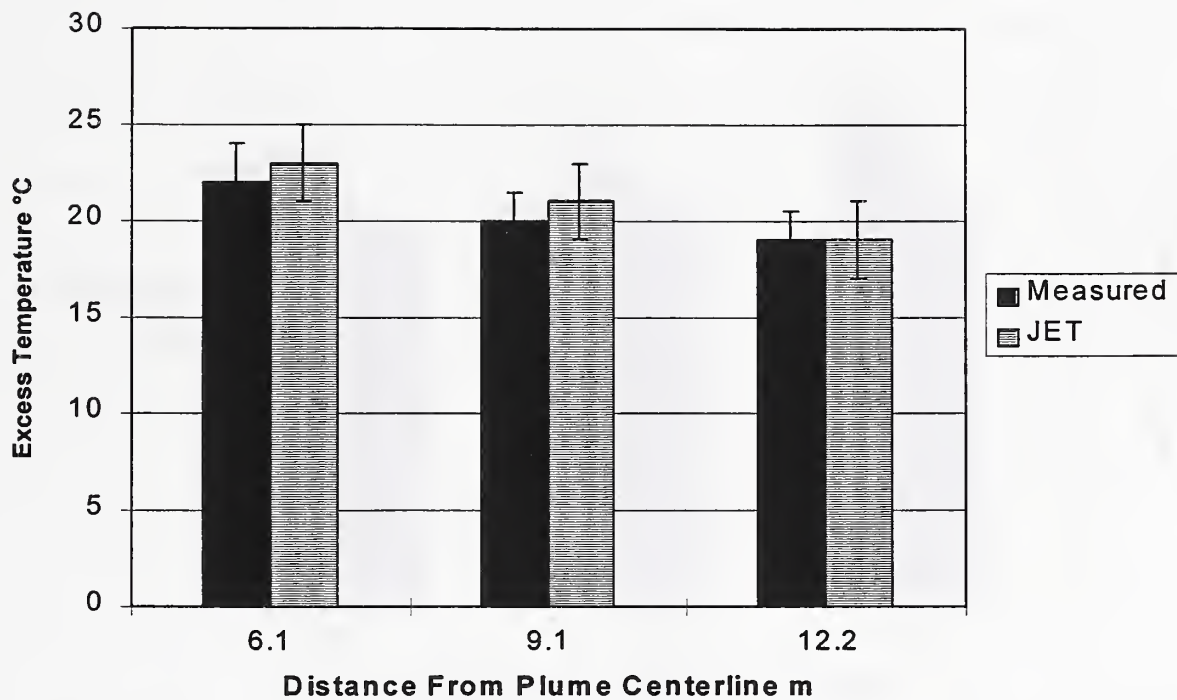
Figure 12 Comparison of measured and predicted ceiling jet temperature for the 22 m high ceiling experiment with a HRR of 2.8 MW. The uncertainty interval for the measurements is based on the measured RMS temperature fluctuation and is equal to ± σ. The uncertainty in the predictions is estimated by varying the radiative fraction by ± 15 %.
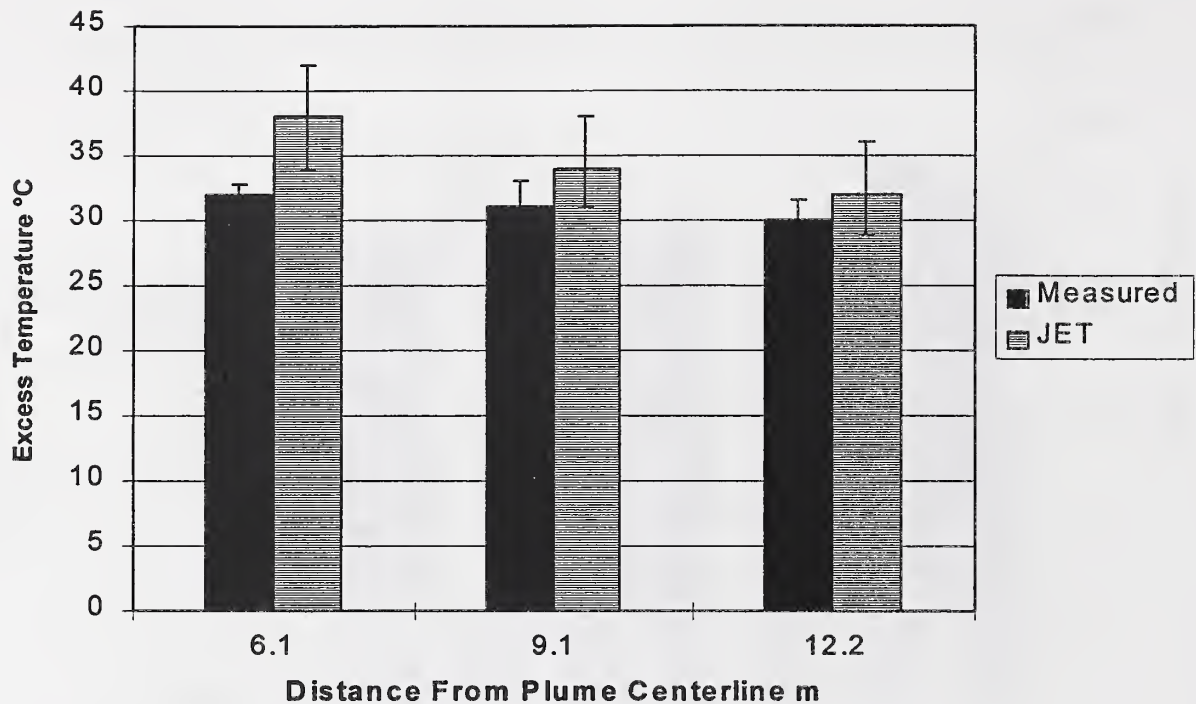
Figure 13 Comparison of measured and predicted ceiling jet temperature for the 22 m high ceiling experiment with a HRR of 4.9 MW. The uncertainty interval for the measurements is based on the measured RMS temperature fluctuation and is equal to ± σ. The uncertainty in the predictions is estimated by varying the radiative fraction by ± 15 %.

Figure 14 Comparison of measured and predicted ceiling jet temperature for the 22 m high ceiling experiment with a HRR of 7.9 MW. The uncertainty interval for the measurements is based on the measured RMS temperature fluctuation and is equal to $\pm \sigma$. The uncertainty in the predictions is estimated by varying the radiative fraction by ± 15 %.

Figure 15 Comparison of measured and predicted ceiling jet temperature for the 22 m high ceiling experiment with a HRR of 14.3 MW. The uncertainty interval for the measurements is based on the measured RMS temperature fluctuation and is equal to ± σ. The uncertainty in the predictions is estimated by varying the radiative fraction by ± 15 %.

Figure 16 Comparison of measured and predicted ceiling jet temperature for the 22 m high ceiling experiment with a HRR of 14.6 MW. The uncertainty interval for the measurements is based on the measured RMS temperature fluctuation and is equal to ± σ. The uncertainty in the predictions is estimated by varying the radiative fraction by ± 15 %.

41

Figure 17 Comparison of measured and predicted ceiling jet temperature for the 22 m high ceiling experiment with a HRR of 15.7 MW. The uncertainty interval for the measurements is based on the measured RMS temperature fluctuation and is equal to ± σ. The uncertainty in the predictions is estimated by varying the radiative fraction by ± 15 %.

Figure 18 Comparison of measured and predicted ceiling jet temperature for the 22 m high ceiling experiment with a HRR of 33 MW. The uncertainty interval for the measurements is based on the measured RMS temperature fluctuation and is equal to ± σ. The uncertainty in the predictions is estimated by varying the radiative fraction by ± 15 %.
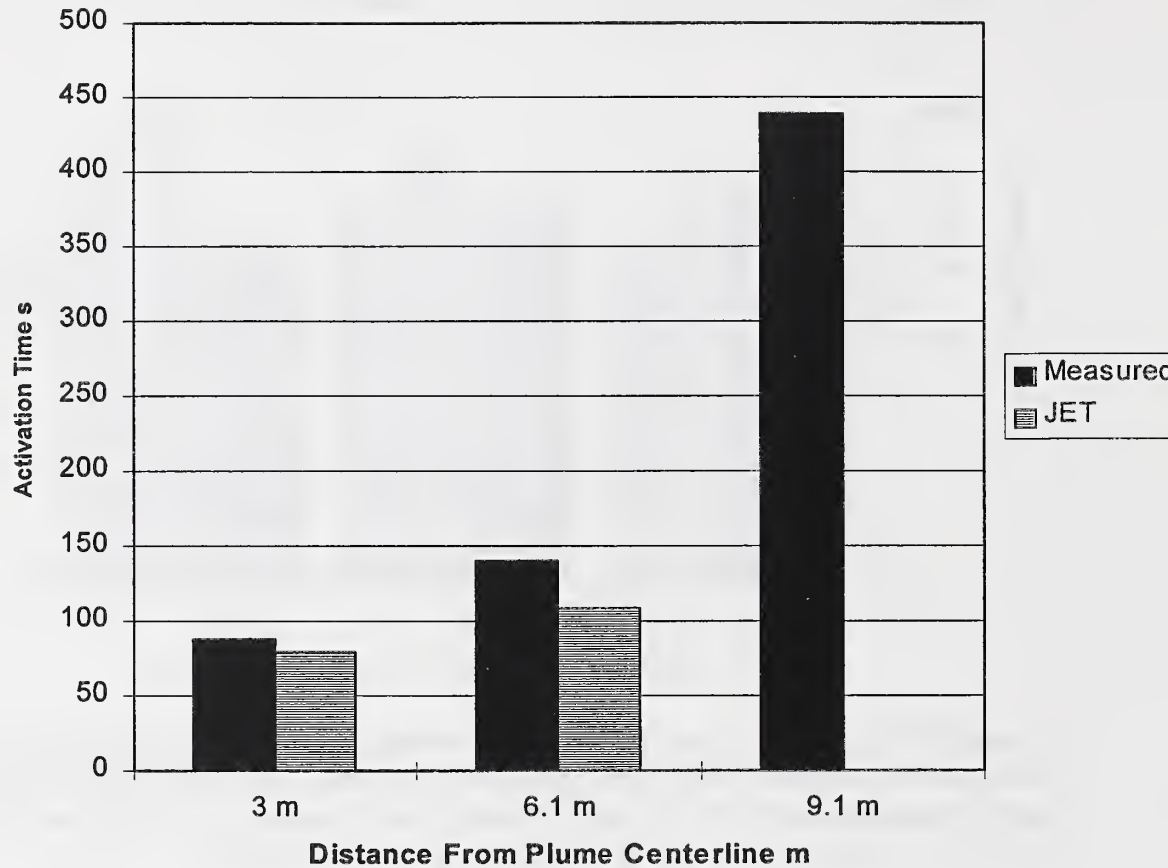
Figure 19 Comparison of measure and predicted activation for sprinklers with 79 °C activation temperature and 35 (m s)$^{1/2}$ RTI for the 15 m high ceiling experiment with draft curtains and a HRR of 7.7 MW.
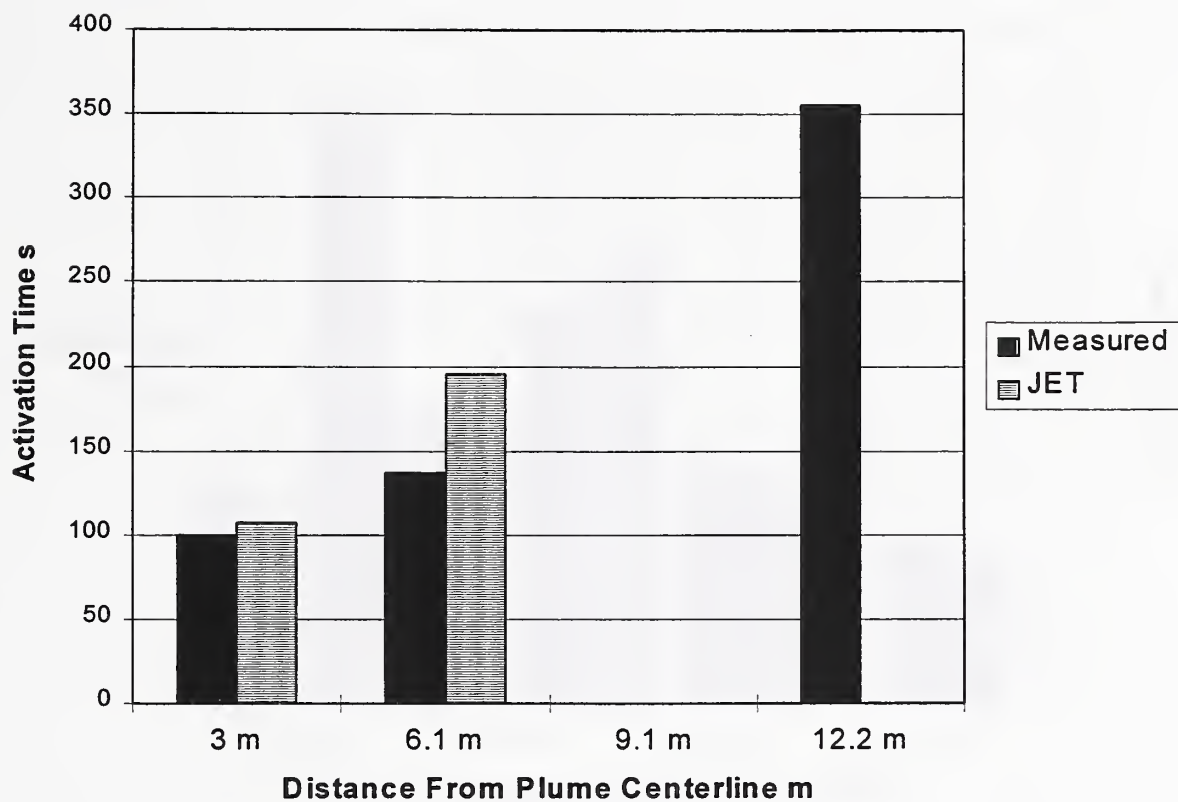
Figure 20 Comparison of measure and predicted activation for sprinklers with 79 °C activation temperature and 35 (m s)$^{1/2}$ RTI for the 22 m high ceiling experiment with draft curtains and a HRR of 14.3 MW.
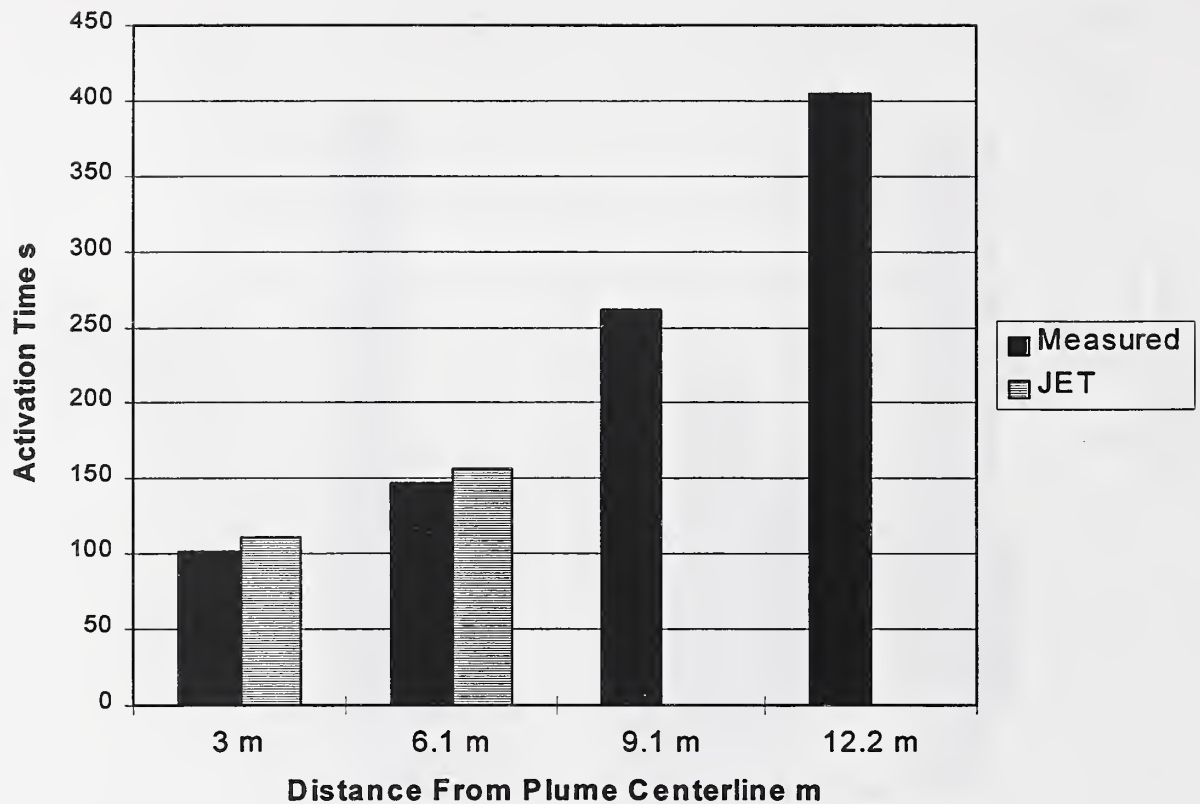
Figure 21 Comparison of measured and predicted activation for sprinklers with 79 °C activation temperature and 35 $(m\ s)^{1/2}$ RTI for the 22 m high ceiling experiment with draft curtains and a HRR of 14.6 MW.
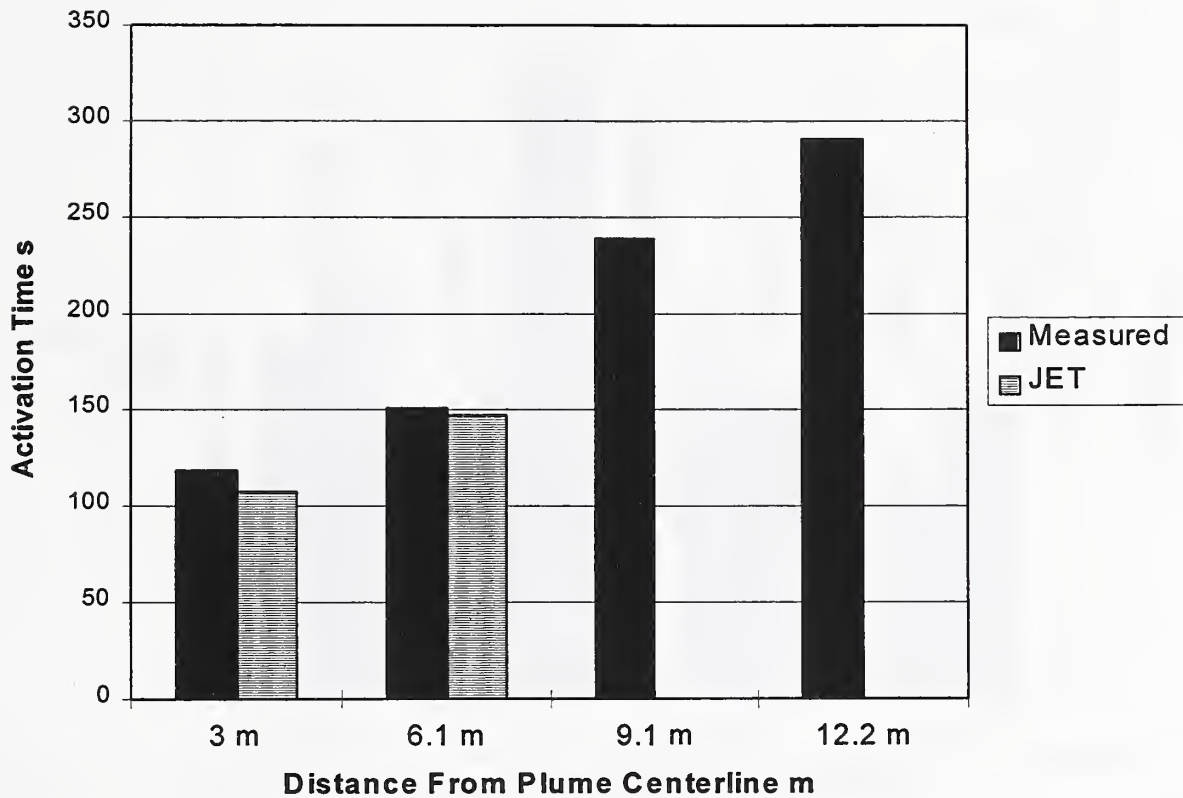
Figure 22 Comparison of measure and predicted activation for sprinklers with 79 °C activation temperature and 35 (m s)$^{1/2}$ RTI for the 22 m high ceiling experiment with draft curtains and a HRR of 15.7 MW.
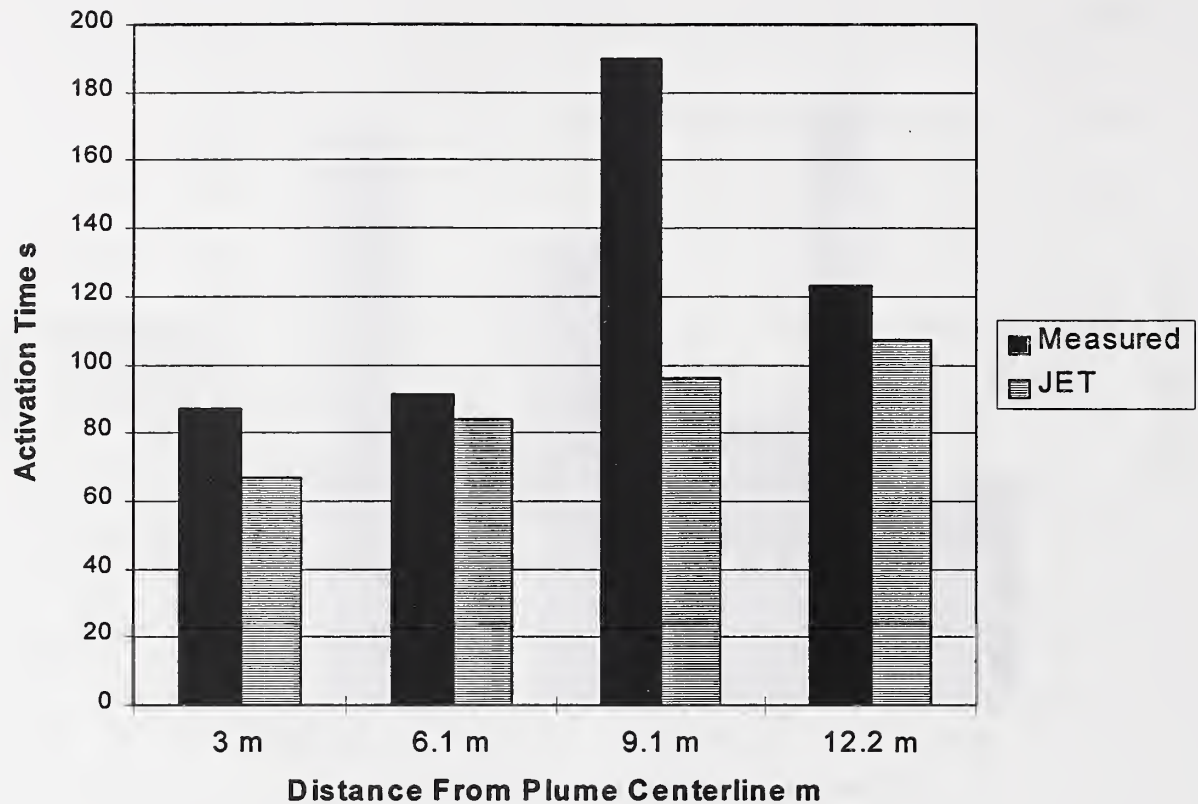
Figure 23 Comparison of measured and predicted activation for sprinklers with 79 °C activation temperature and 35 $(m \, s)^{1/2}$ RTI for the 22 m high ceiling experiment with draft curtains and a HRR of 33 MW.
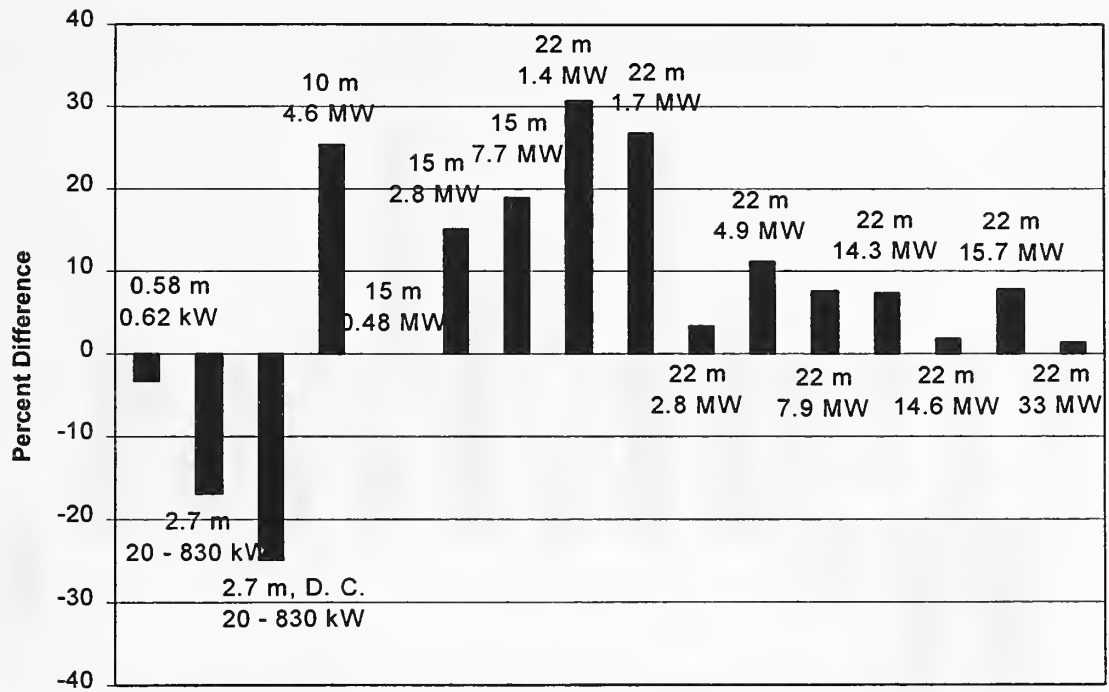
Figure 24 Percent difference between measured and predicted values of the plume centerline temperature. Ceiling heights and HRR are given with each comparison bar.
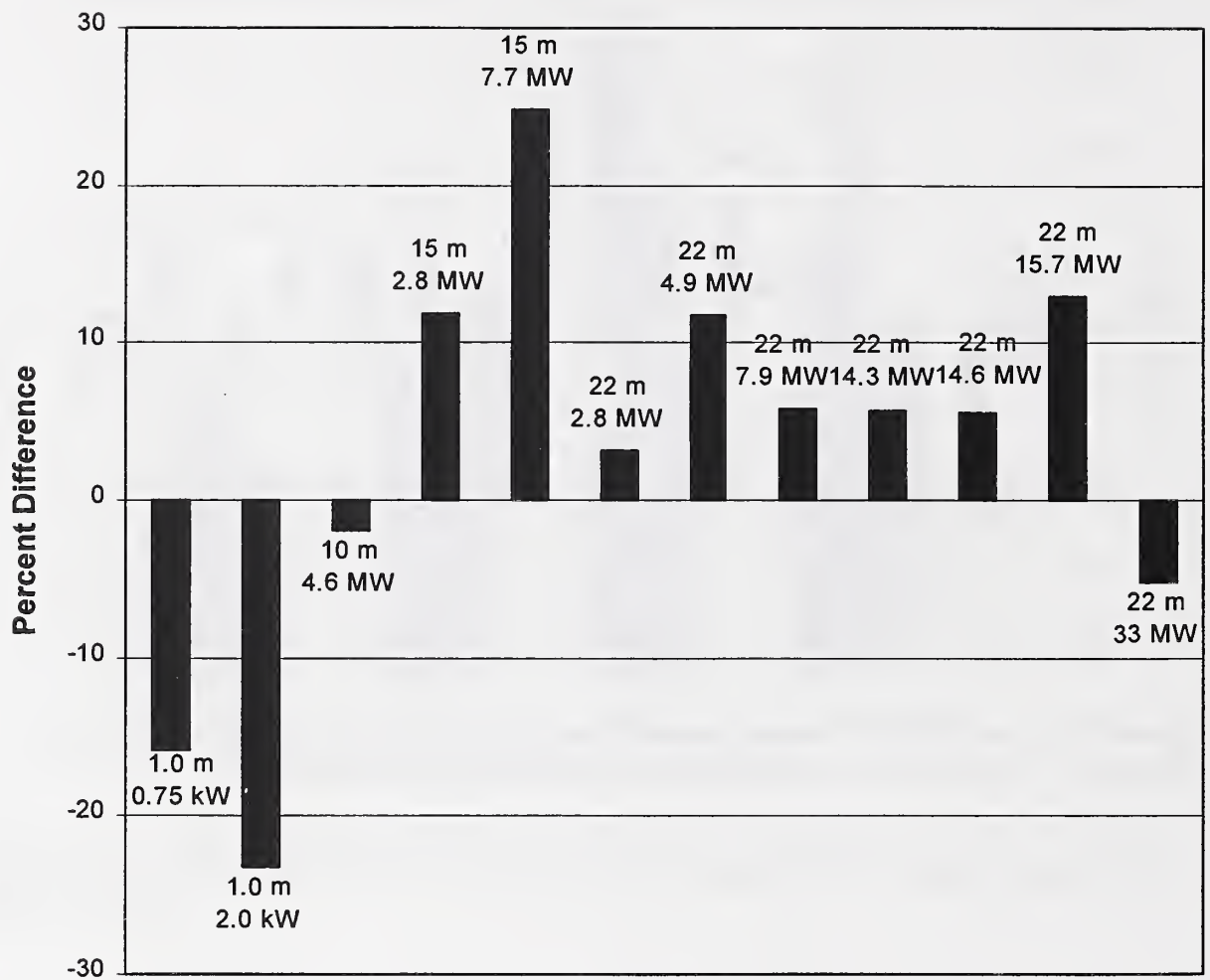
Figure 25
 Percent difference between measured and predicted values of the ceiling jet temperature.
The values shown represent the average over all radial positions for each experiment.
Ceiling heights and HRR are given with each comparison bar.
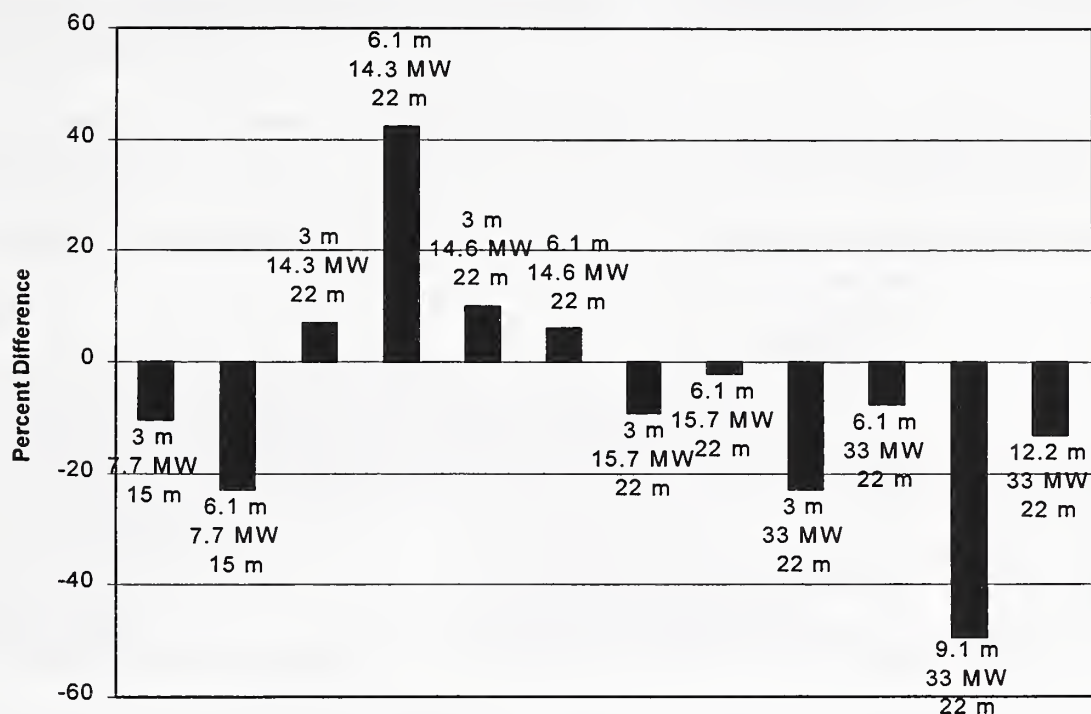
Figure 26 Percent difference between measured and predicted values of the sprinkler activation for distances within 6.1 m of plume center except for the 33 MW fire where the activation comparisons are given out to 12.2 m. Ceiling heights, radial distance from plume centerline, and HRR are given with each comparison bar.

NIST-114	U.S. DEPARTMENT OF COMMERCE	(ERB USE ONLY)	
(REV. 6-93) ADMAN 4.09	NATIONAL INSTITUTE OF STANDARDS AND TECHNOLOGY	ERB CONTROL NUMBER G	DIVISION
MANUSCRIPT REVIEW AND APPROVAL		PUBLICATIONS REPORT NUMBER No. NISTIR 6324	CATEGORY CODE
INSTRUCTIONS: ATTACH ORIGINAL OF THIS FORM TO ONE (1) COPY OF MANUSCRIPT AND SEND TO: WERB SECRETARY, BUILDING 820, ROOM 125		PUBLICATION DATE May 1999	NO. PRINTED PAGES

TITLE AND SUBTITLE (CITE IN FULL)

The Zone Fire Model Jet: A Model for the Prediction of Detector Activation and Gas Temperature in the Presence of a Smoke Layer

CONTRACT OR GRANT NUMBER	TYPE OF REPORT AND/OR PERIOD COVERED

AUTHOR(S) (LAST NAME, FIRST INITIAL, SECOND INITIAL

Davis, W. D.

PERFORMING ORGANIZATION (CHECK (X) ONE BOX)

[X] NIST/GAITHERSBURG
NIST/BOULDER
NIST/JILA

LABORATORY AND DIVISION NAMES (FIRST NIST AUTHOR ONLY)
Building and Fire Research Laboratory/ Fire Safety Engineering Division/864

SPONSORING ORGANIZATION NAME AND COMPLETE ADDRESS (STREET, CITY, STATE, ZIP)
National Aeronautics and Space Administration/NASA Headquarters/Office of Safety and Mission Assurance

PROPOSED FOR NIST PUBLICATION

[ ] JOURNAL OF RESEARCH (NIST JRES)	[ ] MONOGRAPH (NIST MN)	[ ] LETTER CIRCULAR
[ ] J. PHYS. & CHEM. REF. DATA (JPCRD)	[ ] NATL. STD. REF. DATA SERIES (NIST NSRDS)	[ ] BUILDING SCI. SERIES
[ ] HANDBOOK (NIST HB)	[ ] FEDERAL INFO. PROCESS. STDS. (NIST FIPS)	[ ] PRODUCT STANDARDS
[ ] SPECIAL PUBLICATION (NIST SP)	[ ] LIST OF PUBLICATIONS (NIST LP)	[ ] OTHER
[ ] TECHNICAL NOTE (TN)	[X] INTERAGENCY/INTERNAL REPORT (NISTIR)	[ ] –

PROPOSED FOR NON-NIST PUBLICATION (CITE FULLY):   [ ] –U.S.   FOREIGN– [ ]

PUBLISHING MEDIUM:	[X] PAPER	[ ] DISKETTE	[ ] CD-ROM	[ ] WWW	[ ] OTHER

SUPPLEMENTARY NOTES

ABSTRACT (A 2000-CHARACTER OR LESS FACTUAL SUMMARY OF MOST SIGNIFICANT INFORMATION. IF DOCUMENT INCLUDES A SIGNIFICANT BIBLIOGRAPHY OR LITERATURE SURVEY, CITE IT HERE. SPELL OUT ACRONYMS ON FIRST REFERENCE.) (CONTINUE ON SEPARATE PAGE, IF NECESSARY.)

The zone model JET is a two-zone, single compartment computer model designed to predict the plume centerline temperature, the ceiling jet temperature and the ceiling jet velocity produced by a single fire plume. The impact on the upper layer due to the presence of draft curtains, ceiling vents and thermal losses to the ceiling are included in the model. Ceiling mounted fusible links and link actuated ceiling vents can be included in the model calculations. The unique feature of this model is that the characteristics of the ceiling jet depend on the depth of the hot layer.

KEY WORDS (MAXIMUM OF 9; 28 CHARACTERS AND SPACES EACH; SEPARATE WITH SEMICOLONS; ALPHABETIC ORDER; CAPITALIZE ONLY PROPER NAMES)
ceiling jet; ceiling vents; computer models; draft curtains; fire experiments; fire models; heat detectors; sprinkler activation

AVAILABILITY:

[X] UNLIMITED   [ ] FOR OFFICIAL DISTRIBUTION - DO NOT RELEASE TO NTIS
ORDER FROM SUPERINTENDENT OF DOCUMENTS, U.S. GPO, WASHINGTON, DC 20402

[X] ORDER FROM NTIS, SPRINGFIELD, VA 22161

NOTE TO AUTHOR(S): IF YOU DO NOT WISH THIS MANUSCRIPT ANNOUNCED BEFORE PUBLICATION, PLEASE CHECK HERE. [ ]